PCCP

ROYAL SOCIETY OF CHEMISTRY

TUTORIAL REVIEW

View Article Online
View Journal | View Issue

Cite this: *Phys. Chem. Chem. Phys.*, 2025, **27**, 18062

Importance of chirality in the self-organizing peptides – from single molecules to functional supramolecular structures

Agata Chotera-Ouda, [ab] Katarzyna Trzeciak [a] and Marek J. Potrzebowski *[a]

Received 24th April 2025,
Accepted 7th August 2025

DOI: 10.1039/d5cp01562f

rsc.li/pccp

Chirality plays a key role in the self-assembly of peptides, influencing their structural and functional properties from the molecular to the supramolecular level. The stereochemistry of peptides determines their assembly pathways, leading to the formation of well-defined nanostructures such as tubes, wires, helices, fibers, sheets, and gels. This chiral self-assembly not only determines the mechanical and optical properties of the resulting materials but also influences their biological interactions and functionality. Understanding and controlling chirality in peptide systems is essential for the design of advanced biomaterials with tailored properties for applications in nanotechnology, medicine, and tissue engineering. This tutorial review article presents experimental techniques that are dedicated to the study of chiral compounds, allow to determine optical purity, and determine the absolute configuration of the studied species. Techniques for studying higher-order structures of self-assembled peptide systems are also discussed. The role of non-covalent intermolecular contacts in the formation of crystal structures made of heterochiral peptides is presented. The structure and morphology of peptide nanotubes (PNTs), peptide nanowires (PNWs), and other functional peptide devices that arise from the self-assembly and multiplication of chiral structural synthons (CSS), the smallest building blocks, are discussed. Finally, examples of systems belonging to the category of soft materials (peptide hydrogels, organogels) are presented.

[a] *Centre of Molecular and Macromolecular Studies, Polish Academy of Sciences, Sienkiewicza 112, 90-363 Lodz, Poland. E-mail: marek.potrzebowski@cbmm.lodz.pl*
[b] *International Centre for Research on Innovative Biobased Materials (ICRI-BioM)-International Research Agenda, Lodz University of Technology, Zeromskiego 116, 90–924 Lodz, Poland*

Agata Chotera-Ouda

Dr Agata Chotera-Ouda received her BSc and MSc in Biotechnology from Adam Mickiewicz University in Poznan, Poland. She then pursued her PhD degree in Chemistry with Professor Gonen Ashkenasy at the Ben-Gurion University of the Negev in Israel, where she worked on the self-assembly and self-replication of peptides and peptide–DNA conjugates. In 2020 she joined the CMMS PAS as a postdoctoral researcher, studying primarily the crystallization and gelation of cyclic dipeptides. Currently, she is doing her second post-doc in the Nanostructures and Interfaces Group, at the ICRI-BioM, Lodz University of Technology, where she investigates on-surface supramolecular polymers for the fabrication of photoactive devices.

Katarzyna Trzeciak

Dr Katarzyna Trzeciak graduated from the University of Lodz with a PhD in science received in 2012. A long-time Center of Molecular and Macromolecular Studies employee, Polish Academy of Sciences. Winner of the "BIOMAT modern materials and biomaterials" scholarship, Fuga 2 grant leader and co-worker in several research projects financed by the National Science Center. Her interests include mesoporous molecular transporters as drug carriers, effective methods of encapsulating compounds in drug delivery systems, and mechanosynthesis of cocrystals

1. Introduction

In the history of the world and in the development of civilization, there are phenomena that have always, from the very beginning, controlled fundamental processes, but the knowledge of their existence and significance appeared relatively late.[1–3] One of such phenomena is ''chirality'', which defines the key properties of amino acids and nucleic acids, the most important building blocks of living organisms.[4] Chirality, derived from the Greek word ''cheir'', meaning hand, is the property of asymmetry in molecules. Chiral molecules are non-superimposing mirror images of each other, just like our left and right hands. This property is crucial in various biological, chemical, and physical processes and has significant implications in nature.[5] Although many decades have passed since Pasteur's breakthrough discoveries of chirality in the nineteenth century, this scientific platform is still an area of active research.[6–8] Chiral (and non-chiral) building blocks formed and can form higher structures using different types of interactions, which in the first approach can be divided into two groups, covalent bonds and non-covalent interactions.[9] The latter processes are a complex, multi-element phenomenon that is the basis for the development of a very broad strategy called ''molecular self-organization''.[10,11] In this approach, small molecular building blocks spontaneously interact to form hierarchical, functional chiral supramolecular materials. Common key interactions involved in the process include hydrogen bonds, π–π stacking, Coulomb, and van der Waals interactions; thus, in contrast with an approach based on covalent bonding, supramolecular assemblies offer greater responsiveness and tunability.[12] A crucial role in self-organization is played by the hydrophobic effect, which minimizes interactions between nonpolar side chains and water, promoting the aggregation of peptides into ordered structures. The amino acids and short peptides made up of L and D units play a special role among chiral compounds.[13,14] Thanks to their ability to adopt various secondary structures, biocompatibility, and relatively easy design and synthesis, short peptides provide versatile self-organizing soft-matter[15] and have been widely studied in recent years for their implementation in the development of functional smart materials, for example by incorporating synthetic and biological[16–18] or (opto-) electronic moieties,[19,20] providing an effective interface with natural and artificial systems. Moreover, the fundamental knowledge and control over peptide self-assembly can offer crucial information about the formation principles of more complex protein aggregation.

Despite the great progress achieved in recent years in the understanding of the molecular basis of homo- and heterochiral peptide organization processes, the rational design and regulation of their definite structure and function remain challenging. In the case of many sequences, the introduction of D-amino acids destroys their original organization, while for some others, the heterochirality has positive effects on the self-assembly and gelation. Hence, increasing efforts have been focused on stereochemical factors that can influence the properties of the final assemblies, and broaden the repertoire of inherent structural determinants, allowing the formation of more diverse, although controllable, architectures.[21]

The aim of this review is to summarize recent findings in the field and highlight the importance of chirality in the self-organization of short peptides. Special focus is given to its effects on the assemblies across different size scales – all the way from atomic to macroscopic characterization. In the following sections, we discuss how the chirality of amino acid residues influences crystal structure and molecular packing, leads to the formation of various self-assembling morphologies, and finally results in materials of different properties, with a particular focus on the supramolecular gels. Upon conclusion, a few crucial remaining questions and future perspectives are also delivered.

Marek J. Potrzebowski

Marek J. Potrzebowski graduated from the Faculty of Chemistry, Technical University of Łódź in 1979. In the same year, he was employed at the CMMS PAS where in 1986 he obtained a doctoral degree and in 1997 a DSC degree. In 2004, he became a Full Professor. In the years 2016–2023, he was the Director of CMMS PAS. In 1987–1988, he spent two years as a visiting researcher at TexasA@M University, College Station (USA). He also completed a scientific internship at the University of Cambridge (UK), the Technical University of Dresden (Germany) and University H. Poincare, Nancy (France). His scientific interests are related to advanced research on solid matter, methodology of solid state NMR, NMR Crystallography, mechanochemistry, drug delivery systems and peptide science. Currently, he is the Head of the Department of Structural Studies at CMMS PAS.

2. Chirality, basic definitions, and methods for distinguishing stereoisomers

Chirality is a fundamental geometric property of molecules and objects that cannot be superimposed on their mirror images, much like left and right hands. It is pervasive in nature, manifesting across scales from molecular structures like amino acids to macroscopic forms and even galaxies.[22] In chemistry, chiral molecules exist as two non-superimposable mirror-image forms called enantiomers, often categorized as ''right-handed'' or ''left-handed'' (Fig. 1. The source of molecular chirality often lies in stereogenic elements, commonly a carbon atom bonded to four distinct groups in a tetrahedral geometry (Fig. 1B).

Specifically, in the case of amino acids, they exist in nature as either L- or D- enantiomers (except of a non-chiral glycine).

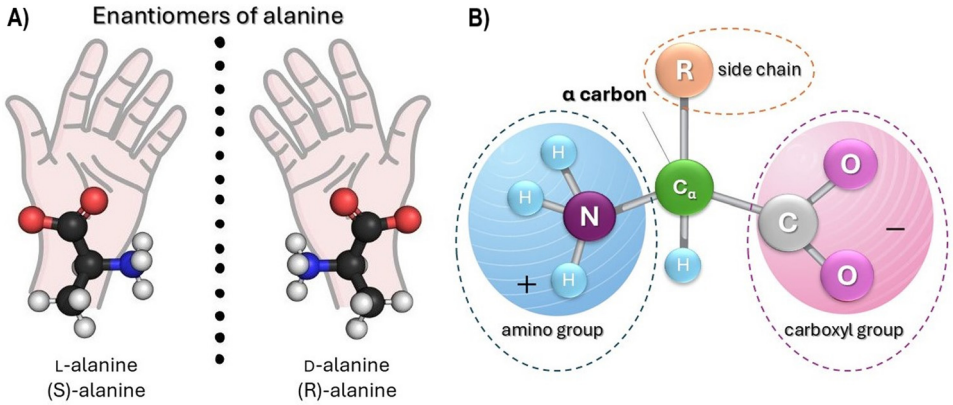

Fig. 1 Stereoisomers of amino acids. (A) Two enantiomers of alanine (L-Ala and D-Ala) that are the mirror reflection of each other. (B) The general structural formula for an α-amino acid.

The two forms are characterized by the different orientations of the four substituents at the α-carbon. In the convention of CIP (Cahn-Ingold-Prelog), the absolute configuration of L amino acids is defined as *S*, while for D amino acids absolute configuration is *R*. The presence of L-amino acids is clearly dominant in the living organisms, resulting in homochirality of the biological world. Taking into account this prevalent use of homochirality in nature, and its preference towards single-handedness of biopolymers, the chirality seems to be critical for a range of complex processes. Nonetheless, the utilization of non-proteogenic D-amino acids in biological molecules, even though rare, seems to play an important role, since naturally existing peptides that contain them include various bioactive peptides such as peptidoglycans, opioid peptides, antibiotics, and cytotoxins, hormones, and others. The incorporation of D-amino acids in peptides for biological applications has been predominantly investigated for increased enzymatic stability and antimicrobial effects.[23] The abovementioned discoveries can be perceived as a motivation for employing D-amino acids in the design of building blocks for functional peptide-based materials, and for comparative analysis of homo- and hetero-chiral self-assembling peptide sequences, as well as their mixtures.

Currently, there are several experimental techniques that allow to determine the absolute configuration of amino acids and their enantiomeric purity (see Fig. 2, left panel). The right panel shows the techniques used to analyze higher-order peptide structures that are formed by short- and long-range intermolecular interactions (bottom panel). These approaches are briefly described below.

2.1. Polarimetry

Polarimetry is a technique that measures the degree of rotation of plane-polarized light caused by chiral molecules. It is well known that the pair of enantiomers has identical physical properties except for how they interact with plane-polarized light. In normal monochromatic light, the electric field oscillates in all directions. When light hits a polarizer, only that part of the light that oscillates in the same plane in which the

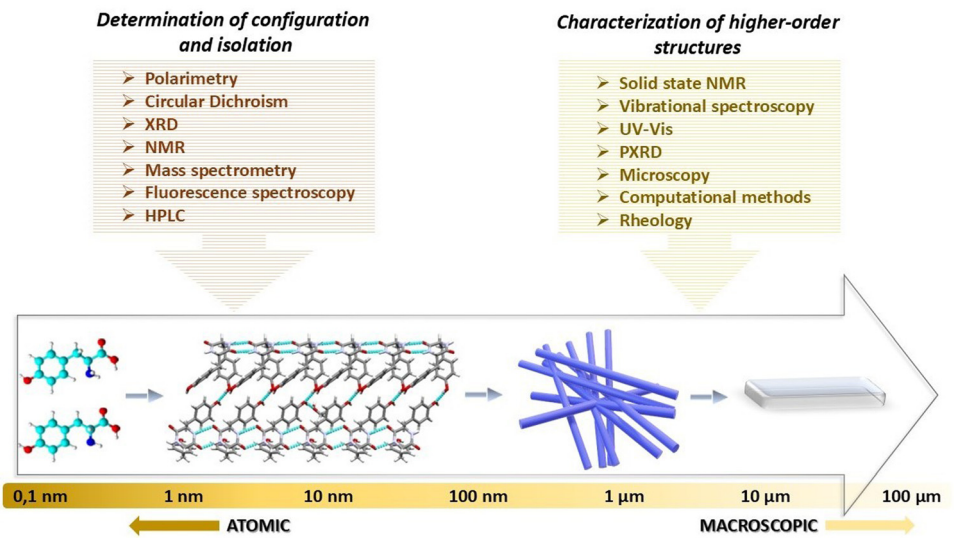

Fig. 2 Schematic representation of the self-assembly of chiral molecules across scales and a list of techniques used for its characterization.

polarizing filter is positioned, can pass through. This plane is called the plane of polarization, and the light is called plane-polarized light.[24] If the substance is optically inactive, the plane of polarized light will not change in orientation. Chiral molecules can rotate the plane of polarized light, and this property is called optical activity. Optical rotation is the degree to which the sample rotates the polarized light. Depending on the direction of rotation of the light, the enantiomer is defined as dextrorotatory (Latin: right, clockwise) and is labeled with the prefix (D) or (+) or levorotatory (Latin: left, counterclockwise) and is designated as (L) or (−).[25] To compare the optical rotation of different compounds under constant conditions, specific rotation is used, a fundamental property of chiral substances expressed as the angle at which the material causes polarized light to rotate at a given temperature, wavelength and concentration.[26–28] Polarimetry determines the ratio of two enantiomers and their purity and concentration. The measurement of the enantiomeric excess (EE), and thus the determination of optical purity, is crucial for pharmaceutical applications because different enantiomers may exhibit divergent physiological effects. Optical purity (expressed as a percentage) is a comparison of the optical rotation of a pure sample of unknown stereochemistry with the optical rotation of a sample of the pure enantiomer. The enantiomeric excess value can range from 0% to 100%. The absolute value of EE is 0% for a racemic mixture and 100% for an optically pure sample.[26,29]

Polarimetry is generally used by pharmacopeias to determine the specific rotation in order to characterize optically pure L-amino acids.[14] The more sensitive type – laser-based polarimetry has been applied in specific rotation measurements of not only amino acids but also di- and tri-peptides.[30]

2.2. Circular dichroism (CD) and vibrational circular dichroism (VCD)

Circular dichroism (CD) is a spectroscopic technique based on differential absorption of left-handed circularly polarized (L-CP) light and right-handed circularly polarized (R-CP) light. In the presence of chiral chromophores, one state of circularly polarized light will be absorbed to a greater extent than the other. CD spectroscopy is an essential analytical technique used to analyze chirality in molecules through their optical activity. Synchrotron radiation circular dichroism (SRCD) spectroscopy offers significant improvements to the well-established method of conventional circular dichroism (cCD) spectroscopy. SRCD takes advantage of the high photon flux available from the light source over a wide range of wavelengths, which results in higher signal-to-noise ratios and also enables the collection of data at lower wavelengths than is possible with cCD spectrometers. Fig. 3 shows the SRCD profiles for L and D alanine.

The obtained CD spectrum does not constitute an intrinsic property of the molecule, but rather depends on the molecular conformation, meaning it is strongly related to the external environmental factors, such as temperature, solvent, *etc*.

Vibrational circular dichroism (VCD) is the extension of circular dichroism spectroscopy into the infrared and near-infrared ranges. The method is mostly applied for the absolute configuration of chiral organic molecules[32] but also provides a possibility to determine the secondary structure of proteins and peptides, complemented by observation of conformational changes. For instance, it was proven to be a useful method for the structural analysis of naturally occurring D-amino acid-containing peptides.[33] Importantly, the VCD spectrum of the chiral molecule can be calculated using an *ab initio* density functional theory (DFT) method.[34] The method is currently gaining popularity due to the low amount of sample required for a measurement and its complementarity with X-ray and NMR methods.

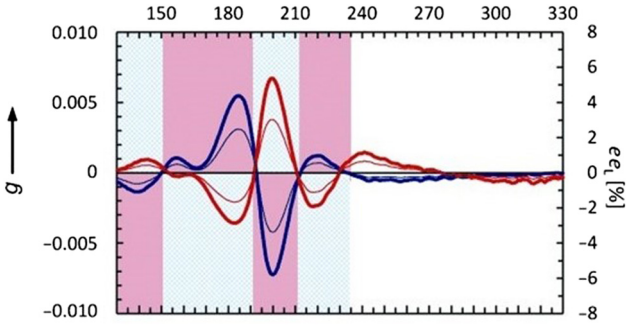

Fig. 3 Anisotropy spectra (thick lines) of isotropic amorphous D-Ala (red) and L-Ala (blue) in the vacuum-UV and UV spectral region. Thin lines represent the corresponding ee_L plots inducible by either left or right circularly polarized light at ξ = 0.9999. Amino acids were sublimated and condensed in the form of isotropic amorphous films. Reproduced and adapted from ref. 31 with permission from John Wiley and Sons, copyright 2012.

2.3. X-ray diffraction (XRD)

X-ray crystallography is the major and routine analytical technique for determining the three-dimensional arrangement of atoms in a crystal, revealing the absolute configuration of chiral molecules.[35–39] If the studied single crystal is of good quality and the diffraction data is unambiguous, the resulting crystallographic results provide accurate and reliable structural parameters that allow researchers to characterize and understand the behavior and function of chiral compounds. The absolute configuration of an optically active molecule, which possesses one or more stereogenic centers, becomes determinable through the effect of X-rays' anomalous scattering (or anomalous dispersion).[35,40] A widely utilized measure in determining absolute configuration is the Flack parameter.[41] In the computation of this parameter, a crystal is treated as if it were twinned by inversion, and the occupancies of the two domains are calculated. This parameter has a physical meaning in the range from 0 to 1. However, experimental outcomes might occasionally deviate from this range due to statistical variations and systematic errors. The Flack parameter assumes a zero value when analyzing an enantiomerically pure crystal in the correct absolute configuration. However, if the crystal structure is inverted, the Flack parameter equals 1.[38,42] Generally, determining the absolute configuration requires a heavy atom in the structure. However, improvements in methods may allow the

absolute configuration to be determined from the ''light atom'' structures (*i.e.* C, O, and N).[39]

2.4. Nuclear magnetic resonance (NMR)

NMR spectroscopy is an effective technique in structural studies and chirality recognition of various chemical compounds,[43–47] which uses the magnetic properties of nuclei.[48] In the case of enantiomers, samples with a single stereogenic center, the active nuclei of NMR are isochronous in an optically inactive environment, so it is not possible to distinguish between them. However, these nuclei are anisochronous in a chiral medium, resulting in different NMR spectra for both enantiomers. There are two general strategies for determining the absolute configuration of compounds. These approaches involve forming a diastereomeric pair of chiral molecules with chiral discriminating agents,[49–51] such as chiral derivatizing agents (CDA)[52–54] and chiral solvating agents (CSA),[55] to obtain two different chemical species with no symmetric relationship. CDAs form covalent bonds with the functional group of the substrate, while CSAs create non-covalent associations, such as hydrogen bonds, ion pairing, dipole–dipole or van der Waals interactions. Among many different chiral discriminating agents, Pirkle's alcohol[56] and Mosher's acid[57,58] are often applied to analyse chiral compounds. The most common NMR technique used to determine the stereochemistry of chiral centres in molecules is ^{1}H NMR.[46,59–63] This is undoubtedly due to the properties of ^{1}H nuclei, such as natural abundance and great sensitivity to environmental modifications.[51] Nevertheless, ^{1}H NMR spectroscopy has certain limitations, and sometimes, analysis of ^{1}H NMR spectra, even small compounds, is complicated. Therefore, ^{13}C NMR is an interesting alternative or good combination with ^{1}H NMR spectroscopy.[64–67] Other nuclei used to determine the absolute configuration of organic compounds are ^{19}F NMR, ^{31}P NMR, and ^{77}Se NMR.[68–74] While applying multinuclear NMR spectroscopy for chiral discrimination and absolute configuration assignment holds promise, it is crucial to assess the reliability of such analyses for specific applications. This evaluation is imperative owing to each element's different nuclear properties and general behaviors.

2.5. Ion mobility mass spectrometry

Ion mobility mass spectrometry (IM-MS) is a powerful analytical technique used to separate and characterize ions based on their size, shape, and charge. When applied to D- and L-amino acids, IM-MS provides valuable insights into their structural properties and stereochemical differences. Mass spectrometry (MS) is a great tool to support chiral analysis in amino acids and peptides. Even though MS is intrinsically ''chirally blind'', because two enantiomers have the same mass and typically show identical mass spectra, some recent developments allow for enantiomer differentiation. The advancements include ion mobility mass spectrometry (IM-MS), photodissociation mass spectrometry, and mass-selected photoelectron circular dichroism (MS-PECD).[75] Specifically, IM-MS has been shown as a promising new technique to achieve rapid isomer separation, and a wide range of IMS-based methods have been described over the years, including chiral ion mobility spectrometry (CIMS),[76] high-field asymmetric waveform ion mobility spectrometry (FAIMS),[77] traveling wave ion mobility and mass spectrometry (TWIM-MS),[78] hybrid trapped ion mobility spectrometry-time-of-flight mass spectrometry (TIMS-TOFMS),[79] and many others. In IM-MS, ions are first generated, usually by electrospray ionization (ESI), and then passed through a drift tube or another mobility separator, where they are subjected to a weak electric field. The ions' drift time, which is influenced by their size and shape, is measured and used to determine their mobility. These measurements are then combined with mass spectrometry to provide high-resolution data on both the mass and structural characteristics of the ions.

For D- and L-amino acids, IM-MS can help distinguish between enantiomers, as they can have slightly different ion mobilities due to subtle differences in their three-dimensional shapes. Although the mass of D- and L-amino acids is identical, their ion mobility can differ, allowing for the potential identification and differentiation of the two forms in complex mixtures. This technique is especially useful in proteomics and biomolecular research, where the precise identification of amino acid stereoisomers is crucial for understanding protein structure, folding, and function.

Recently, a novel automatic analysis was reported, where the measurement is divided into two stages - firstly, chiral derivatization of samples with an (*S*)-naproxen chloride, and secondly, Trapped ion-Mobility MS analysis (TIMS-MS) shown in Fig. 4.[80] Developed protocol provides an interesting possibility for progress in enantioselective high-throughput screenings.

Another new approach, providing access to chirality information applicable to non-volatile molecular materials, such as amino acids, has been proposed by a combination of electrospray ionization (ESI) with the detection of photoelectron circular dichroism (PECD).[81]

2.6. Fluorescence spectroscopy

Fluorescence spectroscopy is fast, relatively inexpensive, and one of the most widely used techniques for studying numerous biological systems. The enantioselectivity, conformational changes, and binding properties of chiral compounds can be easily recognized due to the high selectivity, sensitivity, fast reaction time, non-destructive nature, and versatility of the method.[82–87] Fluorescence measurements make it possible to detect compounds in the systems under study, even if they are present at very low concentrations. Fluorescence is the property of specific atoms and molecules absorbing light at a particular wavelength and then emitting light at a longer wavelength after a short delay, known as the fluorescence lifetime. The emission of electromagnetic radiation is associated with the transition of the molecule between electronic states of the same multiplicity, most often between singlet states S1 → S0.[88] This transition is allowed by the quantum mechanical selection rule and is accompanied by the emission of a photon. Fluorescence emission occurs at a rate of 108 s^{-1}, and the typical fluorescence lifetime is near 10 ns. After absorbing energy in the form of electromagnetic radiation, a molecule has several routes available to return to its ground state. The fluorescence process is

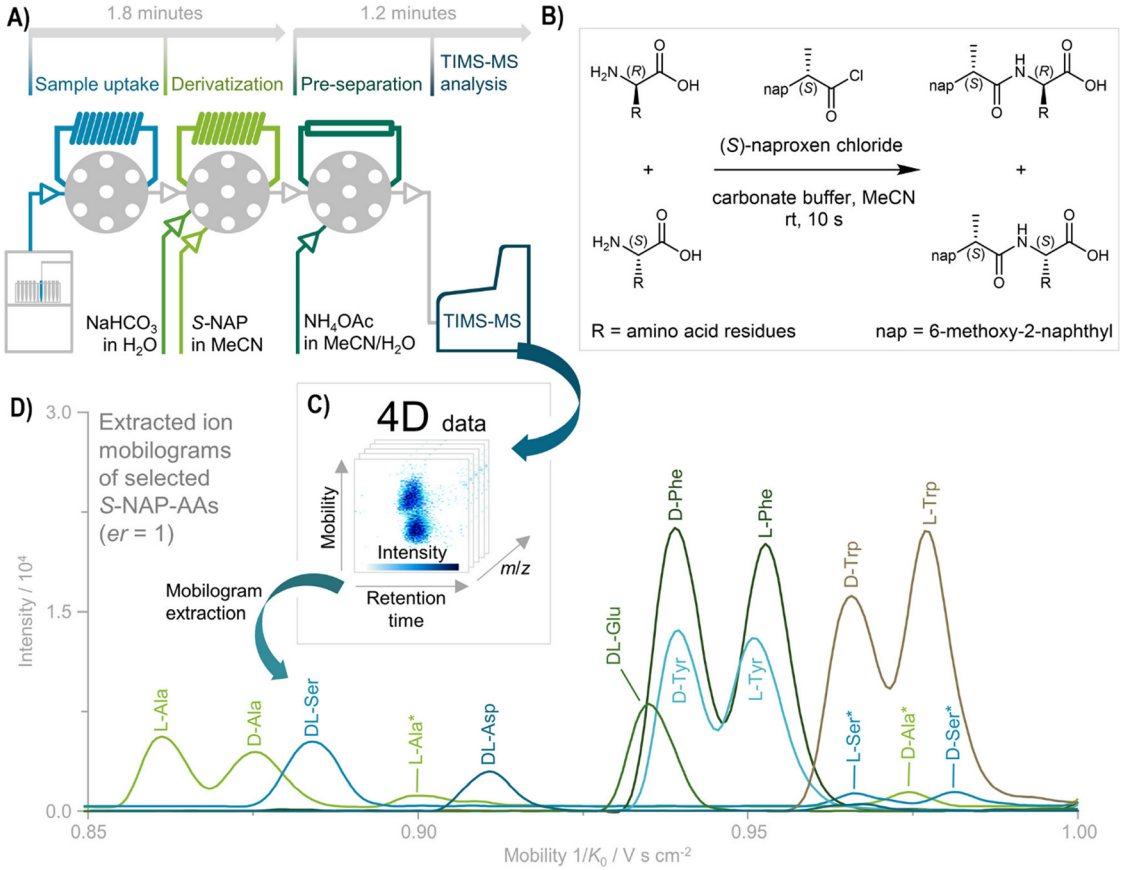

Fig. 4 High-speed chiral analysis of amino acids (AAs); (A) the approach combines automated chiral derivatization with rapid TIMS–MS separation, achieving diastereomer resolution in under 3 minutes per sample. The derivatization process is automated through an autosampler with an integrated chromatography system. After ionization, the AA diastereomers are separated in the TIMS funnel based on their gas-phase mobility; (B) AA enantiomers undergo chiral derivatization using S-NAP; (C) the TIMS–MS system acquires 4D data, capturing retention time, mobility, *m/z*, and intensity; (D) extracted ion mobilograms of S-NAP-AAs from an AA standard mix (er = 1) confirm successful resolution of most D- and L-forms as deprotonated ion species. Ser is distinguished after forming a sodium acetate adduct (marked with *). Reproduced and adapted from ref. 80 with permission from American Chemical Society, copyright 2021.

illustrated by the Jablonski diagram,[89] which is often used as a starting point for discussing molecular processes occurring in excited states involving the absorption and emission of light.

2.7. Other methods (kinetic resolution, HPLC, electrochemistry)

Occasionally, other, more or less sophisticated methods are applied in chirality-related research, especially in cases where the isolation of the preferred enantiomer is necessary. This can be achieved not only by a typical diastereomeric or preferential crystallization, but also by kinetic resolution (chemical or enzymatic) or chromatographic resolution.[90] Kinetic resolution is based on different reaction rates of two enantiomers with a chiral catalyst or reagent, resulting in an enantioenriched sample of the less reactive enantiomer. Various types of catalytic strategies might be employed, using either a single organic catalyst or enzyme, or a combination of two or more types of catalysis, such as enzyme-metal, enzyme-organo, enzyme-photoredox, heterobimetallic, and metal-organo.[91] In peptide specifically, since the conversion of L/D-amino is not uniform, it is necessary to examine individual amino acids at each specific site susceptible to isomerization. It can be performed following one of the two chirality determination protocols: a sequence-dependent strategy or a sequence-independent strategy (see Fig. 5). The sequence-dependent strategy can be applied to identify the isomerized position of the amino acid on the sequence, where in the first step, an enzyme digestion is performed, followed by a chromatographic method, such as RP-HPLC, and a mass spectrometry analysis of collected fractions. Next, the sequences are hydrolyzed to amino acids, followed by a coupling to a standard protected amino acid, in order to obtain LL- and DL- dipeptides that are easy to identify due to different retention times.

In a sequence-independent strategy, the analysis starts with a peptide or protein homogenization and separation of the water-soluble and water-insoluble fractions that undergo enzymatic digestion. The digested peptides are then separated and identified by an LC-MS analysis. Finally, their retention times are compared to that of standard synthesized peptides with several possibilities of enantiomer positions.[92]

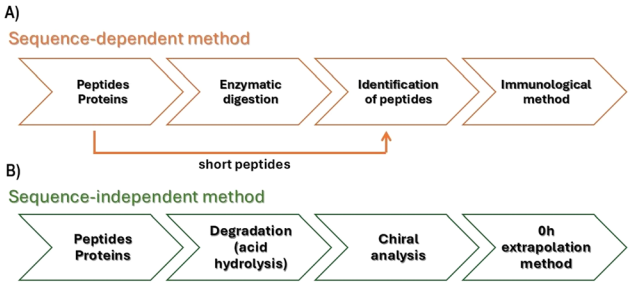

Fig. 5 Flow charts for the determination of D-amino acid residues in peptides and proteins using (A) sequence-dependent and (B) sequence-independent analytical methods.[92,93] Reproduced and adapted from ref. 93 with permission from Elsevier, copyright 2018.

Regarding the direct chromatographic separation of stereoisomers, the conventional HPLC method cannot be successfully applied, thus, chiral chromatography is used to separate compounds into their optical isomers. Nowadays, it is usually achieved by applying the chiral functionalized silica gel as a stationary phase. Some chiral stationary phases (CSPs) can separate a wide range of chiral compounds, while others are useful only for specific types of samples. Commonly used are normal-phase solvents; however, reversed-phase solvents are sporadically applied for specific columns. In different approaches, chiral additives in the mobile phase might be utilized, or derivatization of the analyte to form diastereometric products of the two enantiomers is performed, to allow a standard HPLC separation later on. In addition, capillary and microchip electrophoresis have recently emerged as powerful techniques for the analysis and separation of stereoisomers of various chiral compounds, including peptides.[94]

Out of other separation methods, electrochemistry is sporadically employed for the determination of the chirality of electroactive compounds. Such an approach often requires the development of novel selective and sensitive sensors for the recognition of L- and D- amino acids.[95–97]

Summary of common techniques used to distinguish stereoisomers, along with their typical limitations, presented as Table 1.

3. Experimental methods for studying higher-order structures of self-assembling chiral peptides.

High-resolution detection methods are largely limited by the nature of peptide self-assemblies, due to their poor water solubility and non-crystalline nature, as well as the formation of heterogeneous structures resulting in poly-dispersed samples of different sizes, shapes, and possibly different conformations. Moreover, treating solid-state constructs with solvents can destroy their subtle morphology, leading to misinterpretation of structural data. It is therefore not surprising that experimental methods designed for the study of condensed matter are preferred and give the most reliable results. These techniques can be divided into three groups: spectroscopic methods, diffraction techniques, and microscopic visualizations.

3.1. Spectroscopic methods

3.1.1. Magic angle spinning NMR spectroscopy (MAS NMR). Magic angle spinning (MAS) NMR spectroscopy is a technique used to increase resolution in solid-state nuclear magnetic resonance (NMR) experiments.[98] It is particularly useful for studying solid materials, biomolecules such as peptides and proteins,[99–101] as well as complex heterogeneous systems in which conventional NMR in solution fails due to broad spectral lines caused by dipolar interactions and anisotropic effects. Since the molecular packing of chiral amino acids and their racemic mixtures is usually different, MAS NMR techniques have found a plethora of applications in the study of heterochiral crystal systems.[102] In addition, MAS NMR is an invaluable tool for the analysis of subtle differences at the molecular level in higher-order solid peptide structures and changes forced by the disruption of the stereochemistry of building units.

During the MAS NMR measurement sample is spun rapidly at an angle of 54.74° relative to the applied magnetic field (B_0) (See Fig. 6).[103,104] This angle corresponds to the magic angle, where the second-order Legendre polynomial $(3\cos^2\theta - 1)$ vanishes, reducing dipolar broadening and chemical shift anisotropy (CSA). Typically, the sample is packed in a rotor and spun at speeds ranging from a few kHz to over 100 kHz. Faster spinning leads to better averaging of anisotropic interactions, yielding sharper spectral lines. Fast sample spinning (over 60 kHz) is in particular important for recording the high-resolution ^{1}H MAS spectra.[105]

One of the greatest weaknesses of NMR spectroscopy is the low sensitivity of the measurements. This problem is especially acute when ''rare'' spins are studied. This group includes such nuclei as ^{13}C and ^{15}N important from the point of view of structural research of amino acids and peptides. The natural abundance of ^{13}C is approx. 1.1%, for the ^{15}N isotope approx. 0.36%. Sensitivity, which is a critical factor determining the time of measurement of one-dimensional spectra, becomes even more important with multi-dimensional NMR experiments, as experimental time increases with the introduction of additional indirect dimensions. Sensitivity enhancement results in the reduction of experimental time and hence can more efficiently lead to refined structural insight and complex information on molecular dynamics within the NMR time scales.[106]

In the solid state, the sensitivity enhancement for rare nuclei with low gyromagnetic ratio X is often achieved through Cross Polarization (CP).[107] CP provides sensitivity enhancement by transferring polarization from highly abundant protons to X nuclei. Due to the excitation of protons and observation of X nucleus, an increase in S/N is expected, proportional to gyromagnetic ratio γ_e/γ_d (4 for ^{13}C and 10 for ^{15}N), but in real cases, this factor is always smaller. Another benefit of CP is the possibility of reducing a repetition delay due to favourable relaxation properties of ^{1}H nuclei.

In the case when the samples are not fully solid but have some degree of motional restriction, *e.g.* peptides' semi-solids, hydrogels,

Table 1 The techniques for distinguishing stereoisomers

Technique	Description	Limitations
Polarimetry	✓ Measures the angle of rotation of plane-polarized light ✓ Determines optical purity, distinguishes enantiomers ✓ Monitors stereochemical changes in reactions	✓ Cannot distinguish diastereomers or racemic mixtures ✓ Varying conditions, including solvent, concentration, and temperature, can affect the results ✓ Requires precise experimental conditions
Circular dichroism (CD)	✓ Measures differences in absorption of left- and right-circularly polarized light ✓ Provides spectra with a shape and intensity characteristic of each enantiomer, enabling identification ✓ Enables the distinction of enantiomers	✓ The results are strongly dependent on the solvent, temperature, or pH ✓ Requires clean samples ✓ Spectra can be difficult to interpret for complex systems ✓ Sometimes needs support from other techniques
Synchrotron radiation circular dichroism (SRCD)	✓ Enhanced CD technique using intense synchrotron light with a wide wavelength range ✓ Provides a higher signal-to-noise ratio ✓ Enables data collection at shorter wavelengths ✓ Extends applications of conventional CD	✓ Requires synchrotron access ✓ Despite its higher sensitivity, it still has limitations in distinguishing stereoisomers with similar spectra
Vibrational circular dichroism (VCD)	✓ Measures differential absorption of circularly polarized light in the infrared region ✓ Determines the absolute configuration of organic compounds ✓ Provides info on secondary structure and conformational changes in peptides and proteins	✓ Sensitive to the confirmation and environmental conditions ✓ Often needs DFT calculations ✓ Low signal intensity compared to other spectroscopic methods
X-ray diffraction (XRD)	✓ Provides 3D atomic-level molecular structure ✓ Determines absolute configuration	✓ Requires high-quality crystals, which are difficult for large, complex, or unstable molecules
Nuclear magnetic resonance (NMR)	✓ Analyzes chiral compounds by interaction with chiral shift reagents or by forming diastereomers ✓ Determines enantiomeric excess and absolute configuration ✓ Can study various nuclei (proton, fluorine, carbon, selenium)	✓ Requires relatively large amounts of a clean sample (at least a few milligrams) ✓ The analysis of complex spectra can be difficult and time-consuming
Ion mobility mass spectrometry (IM-MS)	✓ Separates ions by size, shape, and charge in a buffer gas under a weak electric field ✓ Distinguishes enantiomers (*e.g.*, D- *vs.* L-amino acids) *via* subtle 3D structural differences affecting mobility ✓ Offers fast, precise, and sensitive chiral analysis with low sample consumption	✓ Requires specialized equipment and expertise ✓ Analyzing complex mixtures can be challenging, as the presence of many similar compounds often complicates spectrum interpretation
Fluorescence spectroscopy	✓ Fast, affordable, sensitive method for studying chiral fluorescent molecules ✓ Enables chirality recognition and determination of enantiomeric excess ✓ Detects compounds at very low concentrations	✓ Not all compounds naturally fluoresce, which sometimes requires labeling or molecular modification ✓ Sensitive to pH, ionic strength, and quenchers ✓ Difficult to distinguish molecules with similar fluorescence properties
Kinetic resolution	✓ Separates enantiomers by selectively reacting one to form a new product ✓ Yields enantiomerically pure compounds ✓ Used to determine absolute configuration ✓ Common in synthesis and chiral analysis	✓ Max. yield for one enantiomer is 50% without recycling ✓ Requires separation of product from unreacted substrate ✓ Often needs advanced variants (*e.g.*, dynamic or parallel resolution).
High-performance liquid chromatography (HPLC)	✓ Separates and quantifies enantiomers using chiral stationary phases ✓ Can use chiral additives or derivatization to form diastereomers for separation	✓ HPLC requires a properly selected methodology ✓ Sometimes it is associated with high costs and the need for laborious optimization of conditions
Electrochemistry	✓ Distinguishes enantiomers and diastereomers by differences in redox potentials	✓ Only for electrochemically active molecules ✓ Differences may be subtle, which can make unambiguous identification difficult

and slurries. High-resolution magic angle spinning (HR-MAS) NMR is a technique of choice. This technique, dedicated to the study of soft matter, enables high-resolution spectra similar to solution NMR while retaining solid-like sample conditions.[108]

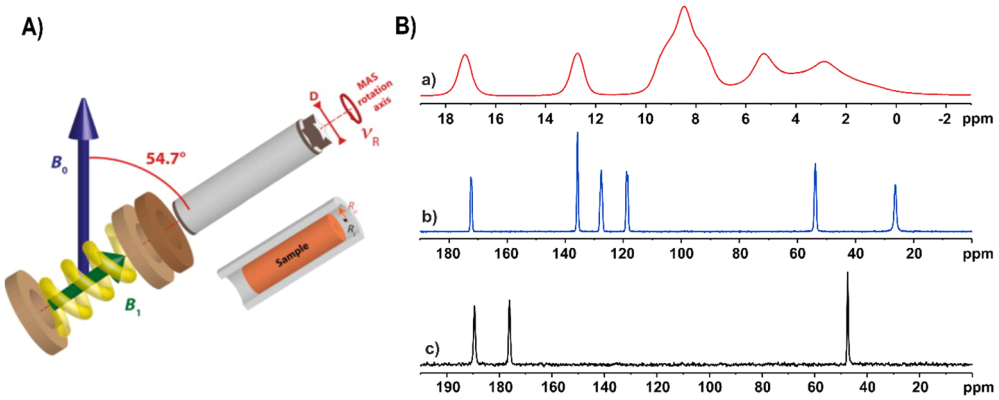

Fig. 6 Schematic representation of MAS NMR measurement and exemplary spectra. (A) Visualization of the idea of magic angle spinning NMR spectroscopy. Reproduced and adapted from ref. 104 with permission from Elsevier, copyright 2014. (B) Solid State NMR spectra of L-histidine HCl recorded with spinning rate 60 kHz (a) ^{1}H MAS NMR (red), (b) ^{1}H-^{13}C CP MAS (blue), and (c) ^{1}H-^{15}N CP MAS (black).

3.1.2. Vibrational spectroscopy. Vibrational spectroscopy allows to identify and classify compounds based on vibrations produced by their bonds, with infrared (IR) and Raman spectroscopy being its two primary types. IR spectroscopy measures the absorption and transmission of infrared light. During the measurement, the sample is irradiated with a broadband of infrared frequencies, and the intensity of the reflected or transmitted radiation is measured as a function of frequency, which can then be used to reconstruct an infrared absorbance spectrum. Some interesting advanced IR methods suitable for chirality and helicity analysis include 2D-IR and ultrafast IR spectroscopy.[109,110] Basic FT-IR (Fourier-transform infrared spectroscopy) does not directly measure chirality, but rather it detects structural features influenced by chirality changes since they affect the formation and strength of hydrogen bonds in peptides. Specifically, heterochiral peptides often exhibit different hydrogen-bonding networks compared to homochiral peptides, which FT-IR can probe.

Raman spectroscopy is another technique used to determine the vibrational modes of molecules, and it relies upon the inelastic scattering of photons, known as Raman scattering. While IR examines the wavenumber at which a functional group has a vibrational mode, Raman observes the shift in vibration from an incident source. Moreover, while IR absorption requires a dipole moment or change in charge distribution to be associated with the vibrational mode, Raman signals occur because of a molecule's polarizability. This results in the complementarity of both techniques. Even though Raman spectroscopy is not regarded as a direct chirality analysis tool, it can be effective in enantioselectivity studies.[111] A relatively new method combining the variability of scattering experiments with the structural sensitivity of chiral spectroscopy is called Raman optical activity (ROA) spectroscopy. ROA measures a small difference in the intensity of Raman scattering from chiral molecules in right- and left-circularly polarized light, providing unique and detailed information about molecular structure and conformational dynamics.[112] ROA has been applied for various studies of peptides and proteins, for example, the decomposition of ROA experimental spectra into calculated spectra of individual conformers, has led to the construction of the two-dimensional potential energy surface ("Ramachandran plot") for the alanine dipeptide Ac-Ala-NHMe.[113]

3.1.3. UV-Vis. UV-Vis spectroscopy is a rapid and non-destructive method for measuring the absorbance of specific chromophores, such as aromatic side chains or peptide bonds, providing valuable structural insights, including information about secondary structures and conformational changes.[114] UV-Vis spectroscopy alone cannot measure chirality directly, as it does not distinguish between enantiomers. However, in the context of chirality studies, it is especially powerful when combined with circular dichroism (CD), as CD reveals details about the chirality and secondary structure of peptides through the differential absorption of circularly polarized light. Recent developments in the area include the design of small-molecule probes that can determine the enantiomeric excess and concentration of amino acids[115] or the exploration of amino acid chiral sensing in visible light, for example, by hydroxypropyl cellulose (HPC) gel.[116]

3.1.4. Powder X-ray diffraction (PXRD). Despite its potential, single-crystal X-ray crystallography (SC-XRD) is not always applicable in the case of peptides because it requires identical conformation of peptide copies throughout a sample and a three-dimensional packing.[117,118] When there are difficulties in obtaining a good quality single crystal of a peptide, another informative experimental method might be applied – powder X-ray diffraction (PXRD). It is a valuable tool for determining whether self-assembled peptide structures exhibit crystalline or amorphous characteristics. Since heterochiral peptides frequently organize into structured formations such as nanofibers, nanotubes, or others, PXRD can detect these by showing distinct diffraction patterns compared to assemblies of homochiral peptides. The diffraction peaks obtained from PXRD yield critical insights into the periodic distances within the peptide structures, including aspects such as layer spacing, helix pitches, and the β-sheets configuration. Furthermore, the data generated by PXRD can substantiate computational models regarding the spatial arrangement of peptides within the assembly, validating the data predicted from molecular dynamics or quantum mechanical simulations.

Peptides that form amorphous or poorly crystalline aggregates present significant challenges for study through PXRD. In such cases, small-angle X-ray scattering (SAXS) and wide-angle X-ray scattering (WAXS) are particularly useful. SAXS analyzes structures at low scattering angles, delivering information about large-scale assemblies and their general shapes, such as bundles of fibrils or layered configurations. In contrast, WAXS examines higher scattering angles, providing insights into short-range molecular ordering and crystallinity, including the arrangement of peptide backbones, hydrogen bonding, and stacking interactions at the angstrom scale. A combination of SAXS and WAXS methods enable hierarchical structural elucidation from the molecular-level details up to the micron scale dimension of the nanotubes, thereby playing a crucial role in the understanding of multi-scale peptide assembly.[119,120]

3.2. Microscopic methods

One of the direct ways to observe the formation of self-assembling structures is through microscopic methods. Among them, transmission electron microscopy (TEM), scanning electron microscopy (SEM), atomic force microscopy (AFM), and scanning tunneling microscopy (STM) are the most popular (see Table 2).

3.2.1. Transmission electron microscopy (TEM) and scanning electron microscopy (SEM). Already 30 years ago TEM was applied to study the influence of molecular chirality on the supramolecular helicity.[121] Since then it has been used in countless studies focused on self-assembled organic morphologies. TEM and SEM allow real-space observation of local structure with high resolution. Over the years the improvements in TEM technique resulted in resolution reaching pictometers and energy resolution to about 100 mV. Nowadays, there are many advanced modes such as HR-TEM, STEM, and 3D tomography offering better ways of imaging, while methods like EDX and similar, allow analysis of element specificity.[122] Even though EM offers a near-atomic-level resolution, it requires drying or freezing of the sample, thus limiting the evaluation of dynamic processes. Moreover, the metal shadowing and electron-beam are other important issues in these imaging options.[123] While comparing TEM and SEM, the main differences lie in the resolution (higher for TEM), and sample preparation (for TEM – samples not thicker than approx. 100 nm), thus it makes SEM perfect for a large-scale overview of present morphologies, while TEM is excellent for more detailed imaging.

3.2.2. Liquid cell electron microscopy (LC-EM). Recently efforts have been focused on ways to overcome the limitations in following the dynamic processes by EM. One of them is the development of liquid cell electron microscopy (LC-EM) technique that enables observation of liquid specimens in real time, and has already been used to study the dynamics of organic molecular assemblies. It seems that the development of liquid-phase EM methods, followed by their application in the studies of organic compounds, might truly revolutionize the field.[124] Similarly, another way of progress might be expected in the application of novel cryo-TEM methods to achieve near-atomic to nanometer resolution using single particle analysis,[125,126] as well as cryo-electron tomography.[127] Another great new development in the area of EM imaging is 4D STEM that captures a full 2D diffraction pattern at each pixel position in a STEM, generating a 4D data cube for further analysis, including maps of local crystal orientation, structural distortions, crystallinity, or different structural classes.[128]

In the study of the influence of chirality on the organization of peptides, EM is and will undoubtedly remain the gold standard of imaging. The observed development of well-known new methods, as well as the use of completely new tools, provides increasingly broader possibilities for analyzing structures at both the molecular and supramolecular levels. Moreover, additional possibilities, such as the observation of dynamic processes or 3D imaging, open broader perspectives for studying changes in the created morphologies and even the slightest differences between them.

3.2.3. Scanning tunneling microscopy (STM). STM is a technique that enables the visualisation of atoms on solid surfaces.[129] STM was developed to analyse conductive surfaces; however, shortly after their invention, it was reported that STM could analyse biological samples after they were deposited on conducting substrates.[130,131] STM allows the obtaining of ultra-high resolution images of a sample's surface on the

Table 2 Displays comparison between various types of microscopy applicable for nanoimaging of peptide-based materials

Technique	STM	AFM	TEM	SEM
Resolution	>0.01 nm	>0.1 nm	>0.01 nm	>1 nm
Imaging principles	Tunneling electrons	Inter-atomic forces	Electrons	Electrons
Environment	Air/vacuum	All	Vacuum	Vacuum
Advantages	✓ Excellent resolution	✓ 3D imaging	✓ Good resolution	✓ Good resolution
	✓ 3D imaging	✓ Applicable to conductors and insulators	✓ Possible tomography	✓ Possible tomography
	✓ High temperature range	✓ Low cost	✓ Diffraction	✓ Diffraction
		✓ Height and phase imaging	✓ Imaging in solution	✓ Imaging in solution
Challenges	✓ Applicable to conducting samples	✓ Possible tip artefacts	✓ Only 2D imaging	✓ Low resolution
	✓ Fragile and very expensive	✓ Limited vertical range and magnification range	✓ Expensive	✓ Only 2D imaging
	✓ Time consuming		✓ Radiation damage	✓ Applicable to conducting samples
	✓ Difficult to operate		✓ Difficult sample preparation	✓ Radiation damage

subnanometer scale and has been proven to be a powerful high-resolution technique in studying the chiral recognition and single-step assembly of amino acids or peptides.[132] STM is a natural choice of technique for studying peptide self-assembly due to its high spatial resolution. It allows the study of molecular structures in real-time, meaning that conformational changes or interactions between biomolecules can be observed *in situ*. This affords precious insight into the behaviors and functions of biomolecules in their native state.[133] Moreover, STM can image biomolecules in liquids[134] and other conditions, such as ultrahigh vacuum,[135] atmosphere[136] or gases, without compromising their structures and biological activity, rendering this technique well-suited for studying delicate biomolecules. STM belongs to the family of scanning probe microscopes (SPM), distinguished by using an exceptionally sharp tip to probe the surface of a sample. STM exploits the quantum mechanical phenomenon of electron tunneling, where electrons tunnel from a conductive tip to a conductive surface at a distance below 1 nm.[129] The small tunneling current depends on the tip-surface distance and bias voltage; therefore, these parameters can be optimized for high-resolution surface scanning.[137] Hence, STM can work in two different modes depending on the application. Images can be generated in constant height mode, where the tip is scanned at a fixed height above the sample surface, and changes of the tunneling current are measured, allowing for rapid scanning of smooth surfaces. Alternatively, the constant current mode is used for highly rough samples, and then the tip also scans perpendicular to the surface to maintain the given tunnel current. This mode is more time-consuming but can be used even on irregular surfaces.[137] Undoubtedly, the key advantage of STM is its high resolution, which allows the mapping of surface topography and electronic properties with much greater detail compared to other microscopy techniques. Moreover, the analysis necessitates only a few micrograms of the sample, which can usually be used for further testing. Additionally, STM can work in various environments from zero Kelvin to several hundred degrees Celsius.[138] STM can be demanding because it requires stable, clean surfaces, sharp conductive tips, and low vibration levels. Despite some limitations, STM is an effective and important tool in studying self-assembling peptides.

3.2.4. Atomic force microscopy (AFM). AFM was developed almost four decades ago, as a way to image objects in nanometer resolution. Thus, for many years now it is one of the standard imaging options in self-assembly studies, providing not only great visuals of the structures but also a lot of information about their physicochemical properties, such as topography, mechanical strength, or dynamics. There are two methods of AFM – a standard dry mode, widely used for many studies over the years, and *in situ* AFM – a method allowing direct observation without drying. The second is especially important for imaging hydrogels and other wet peptide-based soft matter and can be efficiently combined with rheological measurements of the material.[123] One of the new advances called High Speed AFM (HS-AFM) offers high-resolution imaging of fast dynamic processes, such as the assembly and disassembly of peptides. Even though HS-AFM has been previously applied to follow dynamics in biological systems, just recently started to get attention in the field of synthetic supramolecular chemistry.[139,140] An example of the next step in its advancement is the development of HS Bimodal AFM which allowed obtaining high-speed nanomechanical mapping of the collagen growth.[141]

3.2.5. Other microscopic techniques. Sporadically, other microscopy techniques are used for imaging of self-assembly process. One of them is confocal laser scanning microscopy (CLSM) that offers much better resolution than a traditional fluorescence microscope, is not limited by drying or freezing, can be used to obtain 3D images, and allows to follow the dynamic processes.[140] Some powerful types of CLSM with super-resolution have been developed, including stimulated emission depletion microscopy (STED) and a group of techniques known as single-molecule localization microscopy (SMLM).

There are also promising results coming from the development of advanced techniques combining microscopy and spectroscopy methods, such as Raman and Fourier transform infrared (FTIR) imaging.[142,143]

3.3. Computational methods

In recent years, extensive research has focused on computational approaches to study the self-organization and self-assembly of peptides, with molecular dynamics (MD) methods being particularly powerful and frequently applied. Since self-assembling peptides can form various nanostructures, the ways to virtually screen and predict their behavior are of utmost importance. The predictive tool for self-assembly of homochiral dipeptides[144] and tripeptides[145] have been already explored, and involve mostly the coarse-grained MARTINI force field molecular simulations[146,147] The described protocol offers a rapid determination of whether a given peptide sequence is likely to aggregate, whereas longer and larger simulations can be performed after initial screening to obtain more insights into the mechanism of formation of those systems identified as having a potential for self-assembly. The stable conformations accessible to 7- to 10-residues macrocyclic peptides composed of L- and D-amino acids were characterized through near-exhaustive backbone sampling, followed by sequence optimization and energy landscape analysis, yielding over 200 design predictions.[148] The computational design of peptides and peptide macrocycles, including those of mixed chirality, has also been achieved by the Rosetta design software.[149]

One of the novel approaches for conducting MD simulation of various molecular nanostructures, is the so-called molecular dynamics (MD) manipulator, which allows efficient assembly of simulated molecular structures, taking into account the chirality of molecular components, using external force actions.[150,151] The replica exchange molecular dynamics (REMD) technique has also been utilized to determine the morphologies and diversity of self-assembled peptides, including the heteropeptides.[152,153]

In the last few years, novel methods based on artificial intelligence (AI) and deep learning are gaining increased attention for various peptide-related predictions,[154–156] and they are

expected to be a very helpful tool for studies of the heterochiral assemblies.

3.4. Rheology

Rheology is the study of deformation and flow behavior. Self-assembly of peptides often leads to the production of new soft matter, most often in the form of gels. Such materials can be characterized from various angles through rheological tests, describing and comparing their strength, viscosity, deformation, thixotropy, and others. Peptide-based materials are characterized by viscoelastic properties, which are measured in oscillation tests, where one of the most important parameters is the storage modulus G' that represents the elastic portion of the viscoelasticity, thus represents the solid-state behavior of the sample, and the loss modulus G'' that characterizes the viscous part, often seen as the liquid-state behavior. The two properties, monitored against time, frequency, and strain, give insight into gelation kinetics that, together with the general stiffness, directly impact the final application of the material.[157] Rheology offers valuable insights into injectability or thixotropy—a material's ability to shear thin under high shear strain, followed by the recovery to a solid-like material upon removal of high shear.[158] Investigating the kinetics of gel recovery and the underlying restoration mechanisms is an interesting aspect in rheological investigations and is especially crucial for the development of peptide-based injectable therapies.[157]

In peptide-based gel research, the chirality of amino acids plays a pivotal role in determining the material's mechanical properties. Different gel types may be created with altered stiffness, distinct response to changes in concentration, alternated gelation dynamics, and in some cases, a single change in chirality may completely prevent gelation. Therefore, understanding the relationship between peptide hydrogel structure and bulk mechanical properties is one of the central challenges in this field. Thus, to tackle this, rheological studies – essential for characterizing gel behavior – should always be supplemented by structural studies using microscopy and spectroscopy. For example, techniques that integrate rheology with microscopy or scattering have been employed to explore the behavior of shear-thinning gels during and after shear flow.[157] As research advances, there is a growing focus on understanding the interplay between mechanical and morphological properties, especially in the context of chirality-related studies. Specifically, rheological measurements are used in combination with other techniques to draw conclusions about the atomic-level changes in chirality and their influence on the final properties on a macroscopic level. A multidisciplinary strategy combining rheological, structural, computational, and biological methods is essential to uncover the full impact of chirality on peptide-based gels.

4. Self-assembly of homo- and heterochiral peptides

4.1. Molecular crystals of peptides

The crystal structure of a material is one of the highest forms of organization of condensed matter with a well-defined nature of nonbonding interactions. In many cases, the structural information obtained from X-ray studies of single crystals for amino acids and small peptides is taken as reference data that can be extrapolated to the interpretation of higher-order peptide assemblies. Solid state structural studies of amino acid chirality began at the end of the 19th century when O. Wallach tried to answer the question of why DL-alanine crystals are denser than L-alanine crystals. Systematic studies of chiral crystals have led to the conclusion that heterochiral molecules pack together more efficiently than homochiral molecules.[159] This statement, known in the literature as Wallach's rule, has been critically evaluated several times.[160] An attempt to explain the correlation between crystal packing and the stability of chiral and racemic proteogenic amino acids on the basis of experimental results and theoretical calculations was made by J. D. Dunitz and A. Gavezzotti.[161]

It is well known that crystals are organized according to specific rules with a hierarchy of intermolecular interactions.[162] The list of these interactions includes: electrostatic interactions between charged moieties, hydrogen bond interactions, van der Waals interactions, and π–π arrangement. These interactions play different roles in the hierarchical process of self-organization, moving at various scales, from elementary molecules to higher-order structures (see Fig. 7). The presence of stereogenic peptide centers can significantly interfere with the nature of these interactions. Below are some examples showing the importance of cumulative effects (non-covalent interactions, chirality) responsible for peptide self-assembly.

The most spectacular observations on the effect of chirality on the morphology of peptide crystals are related to structural studies of the phenylalanine-phenylalanine (Phe-Phe) dipeptide. Self-assembling of Phe-Phe first discovered and described by Gorbitz *et al.*,[163] was intensively studied by Gazit[164–166] and many other research groups over the years.[167–171] This model has become a reference sample and a "workhorse" used to understand the fundamental processes that define the final form of matter. Fig. 8 shows the molecular packing for the dipeptides L-Phe-L-Phe and D-Phe-D-Phe constructed from experimental data of their crystallographic structures obtained by X-ray methods and deposited in the crystallographic database of the Cambridge Crystallographic Data Center (CCDC).

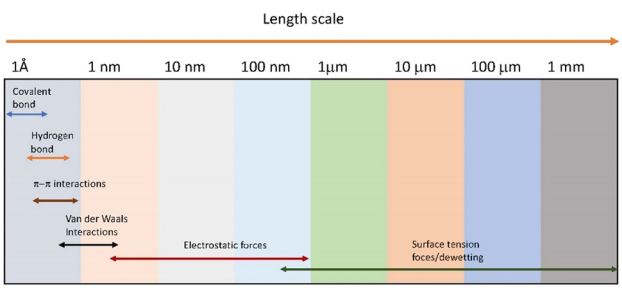

Fig. 7 Comparison of the range of intermolecular interactions involved in the process of peptides self-assembly. Each type of interaction contributes differently to the hierarchical assembly across various scales, from basic molecular units to higher-order structures.

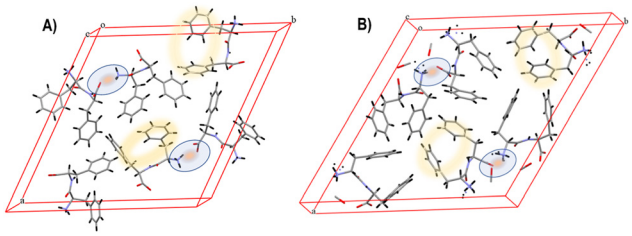

Fig. 8 (A) Molecular packing of L-Phe-L-Phe (CCDC 163340) and (B) D-Phe-D-Phe (CCDC 1853771) crystals.

Table 3 Lattice cell parameters for L-Phe-L-Phe and D-Phe-D-Phe PNT (from ref. 140,163,172 according to CCDC[174])

	L-Phe-L-Phe	d-Phe-d-Phe
Space group	$P6_1$	$P6_5$
a, Å	24.0709(13)	23.9468(14)
b, Å	24.0709(13)	23.9468(14)
c, Å	5.4560(4)	5.4411(2)
V, Å^3	2737.7(3)	2702.2(2)

(These data correspond to No. CCDC 163340 for L-Phe-L-Phe and No. CCDC 1853771 for D-Phe-D-Phe).[172,173] In both cases the crystal structures contain six Phe molecules, and it is formed by a total of 258 atoms, while the space groups of these enantiomers are different: $P6_1$ space group for L-Phe-L-Phe and $P6_5$ for D-Phe-D-Phe. The basic structural information are collected in Table 3.

It is worth noting that both crystals are organized according to the hierarchical rules described above. The zwitterionic nature of the dipeptide is correlated with long-range electrostatic interactions. Aromatic–aromatic interactions force a synclinal arrangement of the main skeleton, which opens up the possibility of creating a higher-order structure by means of hydrogen bonds. External stimuli and environmental factors can significantly affect molecular packing and disrupt the hierarchy of non-covalent interactions. Fig. 9 shows the molecular packing of L-Phe-L-Phe dipeptide crystalized in methanol.[175] The differences between hydrate and methanol solvate are apparent. The latter system crystallizes in orthorhombic space group $P2_12_12_1$ with Z' equal 1 and Z = 4. The cell volume is 1937.25 Å^3, much less compared to the hydrate. The size of the unit cell is a = 4.866 Å, b = 17.275 Å, c = 23.046 Å. The most important difference is the conformation of the dipeptide. In the case of methanol solvate, the main skeleton of the dipeptide is present in the form of a stretched chain with phenyl groups on opposite sides. In the crystalline unit, only intermolecular, weak aromatic–aromatic interactions are observed. Such a "stretched" conformation defines further possibilities for self-assembly and virtually eliminates the formation of nanotube peptides.

The intriguing example of a correlation between nonbonding interactions and chirality are crystals of racemic mixture D-Phe-D-Phe and L-Phe-L-Phe. The unit cell contains eight molecules (Z = 8) organized in homochiral pairs (see Fig. 10). Crystal crystallizes in the $P2_1$ space group. The size of the unit cell is a = 8.9648(15) Å, b = 30.515(5) Å, c = 11.9680(19) Å, volume is 3273.86 Å^3. The subtle structure of this crystal is controlled by electrostatic interaction, hydrogen bonding, and chirality. These effects have an impact on further self-assembly. The specific character of hydrogen bonding interactions is the reason why the creation of nanowires rather than nanotubes is preferred.

Expanding research on Phe-Phe analogs, the group of Marchesan studied the supramolecular packing modes of heterochiral, aliphatic dipeptides L-Leu-D-Xaa (Xaa = Ala, Val, Ile, Leu).[177] The XRD analyses were performed using synchrotron radiation. L-Leu-D-Ala (CCDC: 2300851) crystallizes as a hydrate with water molecules localized in layers parallel to the ab plane, while the previously reported homochiral analog (L-Leu-L-Ala) forms water channels.[178] The second dipeptide – L-Leu-D-Val (CCDC: 2300852) also crystallizes as a hydrate with a simple solid-state assembly, characterized by the presence of amphipathic layers and water molecules occupying non-interconnected cavities. Interestingly, a homochiral L-Leu-L-Val reported by Görbitz,[179] showed a peculiar crystal packing, being the first linear peptide with Z = 24. The next two dipeptides L-Leu-D-Leu and L-Leu-D-Ile (CCDC: 2300853 and 2300854, respectively), both crystallize as DMSO solvate crystal structures with the guest molecules which occupy channels parallel to the a axis, whereas analyzed earlier L-Leu-L-Leu involves head-to-tail interaction of peptide molecules and segregation of polar and nonpolar regions.[180] All the basic

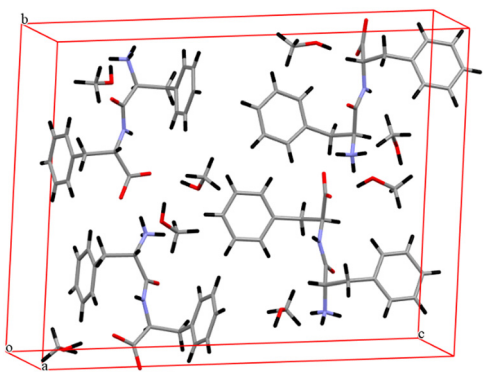

Fig. 9 The molecular packing of L-Phe-L-Phe dipeptide crystalized in methanol (CCDC 994055).

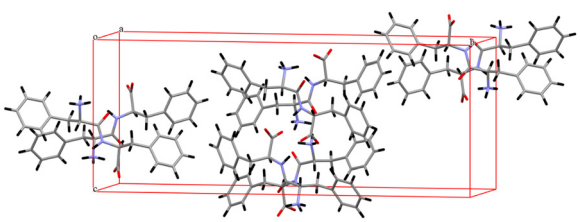

Fig. 10 Molecular packing of racemic mixture D-Phe-D-Phe and L-Phe-L-Phe (CDCC 205941). Reproduced and adapted from ref. 176 with permission from John Wiley and Sons, copyright 2021.

Table 4 Lattice cell parameters for dipeptides: L-Leu-D-Ala (La) dihydrate (CCDC 2300851), L-Leu-L-Ala (LA) tetrahydrate (CCDC 128697), L-Leu-D-Val (Lv) hydrate (CCDC 2300852), L-Leu-L-Val (LV) hydrate (CCDC 1215952), L-Leu-D-Leu (Ll) dimethyl sulfoxide solvate (CCDC 2300853), L-Leu-L-Leu (LL) dimethyl sulfoxide solvate (CCDC 1305438), L-Leu-D-Ile (Li) dimethyl sulfoxide solvate (CCDC 2300854)

	La	LA	Lv	LV	Ll	LL	Li
Space group	$C2$ (5)	$P2_12_12_1$ (19)	$C2$ (5)	$P6_2$ (171)	$P2_1$	$P2_1$	$P2_1$
a, Å	16.704(3)	6.186(2)	19.250(4)	29.212(16)	5.362(11)	5.434(4)	5.583(11)
b, Å	4.766(10)	12.548(4)	6.476(13)	6.4760(13)	14.938(3)	15.712(7)	14.434(3)
c, Å	16.102(3)	19.883(6)	13.049(3)	11.723(9)	11.345(2)	11.275(2)	22.161(4)
α	90°	90°	90°	90°	90°	90°	90°
β	99.05(3)°	90°	103.72(3)°	90°	91.61(3)°	100.41(1)°	92.76(3)°
γ	90°	90°	90°	119.99°	90°	90°	90°

structural information for the abovementioned peptides is summarized in Table 4.

To further broaden the scope of research, Mandal and colleagues published a comprehensive X-ray diffraction study of single-crystal X-ray (SC-XRD) heterochiral Boc-Val-Phe-Phe-OMe tripeptides.[181] In contrast to the previously discussed examples, tripeptide models are protected at both the *C* and *N* ends, which means that they are not zwitterionic systems. It has a significant impact on the organization of the crystal lattice because it eliminates electrostatic interactions as a controlling factor for self-assembly.

Table 5 shows the basic structural information and lattice cell parameters for Boc-Val-Phe-Phe-OMe crystals. Boc-L-Val-D-Phe-D-Phe-OMe crystallized in the monoclinic ($P2_1$) space group and exhibited one molecule in the asymmetric unit. Each subunit was interconnected through an intermolecular H-bond to adopt a parallel beta-sheet structure along the c-axis in the crystalline state. The NH group and oxygen of L-Val of one subunit were intermolecularly H-bonded to the next subunit of the oxygen of urethane and NH of central D-Phe, respectively. Both peptide Boc-L-Val-D-Phe-L-Phe-OMe and Boc-D-Val-L-Phe-D-Phe-OMe crystallized in the triclinic ($P1$) space group and showed one molecule in the asymmetric unit. Each molecule of both Boc-L-Val-D-Phe-L-Phe-OMe and Boc-D-Val-L-Phe-D-Phe-OMe was interlinked through three intermolecular H-bonds to create a parallel beta-sheet structure along b-direction. Peptides Boc-L-Val-L-Phe-D-Phe-OMe and Boc-D-Val-D-Phe-L-Phe-OMe crystallized in orthorhombic ($P2_12_12_1$) space group and exhibited one molecule) in the asymmetric unit. Each molecule of both Boc-L-Val-L-Phe-D-Phe-OMe and Boc-D-Val-D-Phe-L-Phe-OMe was intermolecularly interconnected through three H-bonds to form a parallel beta-sheet structure along *c*-direction. The oxygen of urethane, NH, and oxygen of central Phe of one molecule was intermolecularly H-bonded to the next molecule of the NH and oxygen of Val and the NH of C-terminal Phe, respectively in both Boc-L-Val-L-Phe-D-Phe-OMe and Boc-D-Val-D-Phe-L-Phe-OMe. Next, molecules were self-associated to build a helical sheet-like structure in higher-order packing along a-axis in both enantiomeric peptides Boc-L-Val-L-Phe-D-Phe-OMe and Boc-D-Val-D-Phe-L-Phe-OMe. Fig. 11 shows the molecular structure of models refined by means of X-ray crystallography.

Table 5 Lattice cell parameters for heterochiral Val-Phe-Phe protected peptides: Boc-L-Val-D-Phe-D-Phe-OMe (Vff), Boc-L-Val-D-Phe-L-Phe-OMe (VfF), Boc-D-Val-L-Phe-D-Phe-OMe (vFf), Boc-L-Val-L-Phe-D-Phe-OMe (VFf), Boc-D-Val-D-Phe-L-Phe-OMe (vfF)

	Vff	VfF	vFf	VFf,	vfF
Space group	$P2_1$	$P1$	$P1$	$P2_12_12_1$	$P2_12_12_1$
a, Å	5.0081(2)	4.9397(5)	4.9548(4)	5.0710(2)	5.0543(9)
b, Å	26.9990(17)	10.8307(10)	10.8351(12)	15.1956(6)	15.267(3)
c, Å	11.0196(8)	13.6935(13)	13.6908(16)	37.6927(14)	39.355(7)
V, Å^3	1488.98	724.469	726.851	2904.48	3036.79

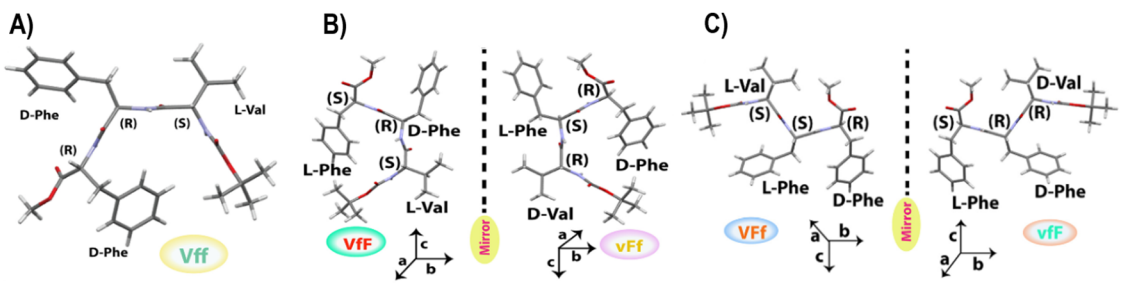

Fig. 11 Crystal structures of different tripeptides: (A) Boc-L-Val-D-Phe-D-Phe-OMe (Vff), (B) Boc-L-Val-D-Phe-L-Phe-OMe (VfF) and Boc-D-Val-L-Phe-D-Phe-OMe (vFf), (C) Boc-L-Val-L-Phe-D-Phe-OMe (VFf) and Boc-D-Val-D-Phe-L-Phe-OMe (vfF). Reproduced and adapted from ref. 181 with permission from John Wiley and Sons, copyright 2021.

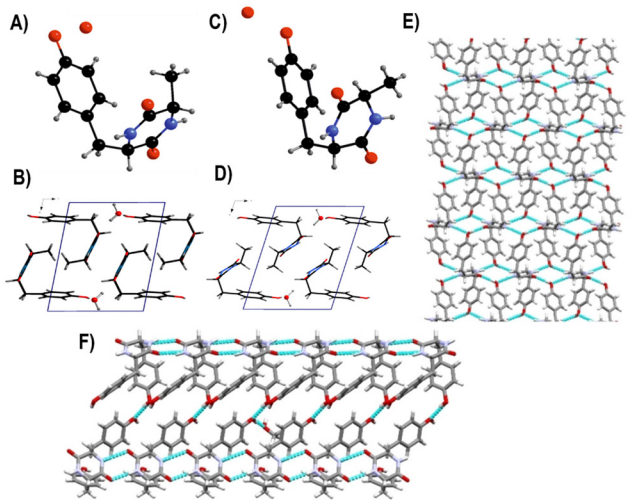

Fig. 12 Molecular packing of (A) Boc-L-Val-D-Phe-L-Phe-OMe (CCDC 2015774) and (B) Boc-L-Val-L-Phe-D-Phe-OMe (CCDC 2015776).

Fig. 12 shows how chirality inversion can dramatically change the arrangement of molecules in the crystal lattice for peptides with different stereochemistry. Fig. 12A displays the molecular packing for Boc-L-Val-D-Phe-L-Phe-OMe, while Fig. 12B shows the molecular packing for Boc-L-Val-L-Phe-D-Phe-OMe sample.

The same group has investigated L/L and L/D amino acid-containing dipeptides, Boc-L-Ile-L-Phe-OMe, Boc-L-Ile-D-Phe-OMe, Boc-L-Ile-L-Phg-OMe (Phg = phenylglycine), and Boc-L-Ile-D-Phg-OMe (Fig. 13A).[182] Fig. 13B shows how stereochemistry and chemical modification affect the solid-state peptide backbone arrangement. The presence of extra methylene ($-CH_2-$) group on the side-chain of C-terminal Phe of Boc-L-Ile-L-Phe-OMe causes a significant deviation of molecular arrangements from that of Boc-L-Ile-L-Phg-OMe. While the molecules in Boc-L-Ile-L-Phe-OMe self-assemble to form a single helix-like architecture, the molecules in Boc-L-Ile-L-Phg-OMe self-associate around a water molecule to form a cylinder-like structure in the crystalline state. Alternatively, the observed supramolecular arrangements of Boc-D-Val-L-Ile-OMe and Boc-L-Ile-D-Val-OMe are similar, but deviate from that of Boc-L-Val-L-Ile-OMe and Boc-L-Ile-L-Val-OMe, due to chirality difference.[183]

Other interesting cases might be found in studies focused on cyclic dipeptides. Investigations have been conducted on the cyclic compounds of Tyr-Ala and Tyr-D-Ala noted as cyclo(L-Tyr-L-Ala) and cyclo(L-Tyr-D-Ala), respectively, and structural differences between them have been noticed (see Fig. 14A–D). In particular, slight differences were observed in the arrangement of water molecules in the hydrophilic channels and the geometry of the diketopiperazine rings.[184] Very recently, structural data for cyclo(L-Tyr-L-Tyr) and cyclo(L-Tyr-D-Tyr) were published. While the cyclo(L-Tyr-L-Tyr) exists in few solid forms that display a network of parallel hydrogen-bonded stripes, promoting a unilateral growth, its D-Tyr containing analog shows a propensity towards a two-dimensional growth (see Fig. 14E and F).[185]

4.2. Higher order structures of self-assembling homo and heterochiral peptides

Self-assembly of peptides refers to the spontaneous organization of peptide molecules into ordered nanostructures or supramolecular architectures driven by non-covalent interactions shortly discussed in Section 4.1. This process results in the formation of well-defined structures with specific functions and properties. The spatial distribution of the residues around the stereogenic center determines the morphology of the final product. Thus, we can conclude that the chiral structural synthon (CSS), which is the smallest basic building block, is responsible for the formation of complex higher-order structures in the process of proliferation (self-organization). This hypothesis can be verified taking as an example molecular structure in the crystal lattice of Phe-Phe dipeptide (see Section 4.1). For L-Phe-L-Phe and D-Phe-D-Phe, where the arrangement of phenyl groups is synclinal, then CSS creates the possibility of formation of peptide nanotubes because the hydrophobic and hydrophilic parts are located in different spaces (Fig. 15).

When such an arrangement is not possible because the solvent forces a different spatial arrangement (*e.g.* L-Phe-L-Phe crystallized from methanol) and the arrangement of phenyl

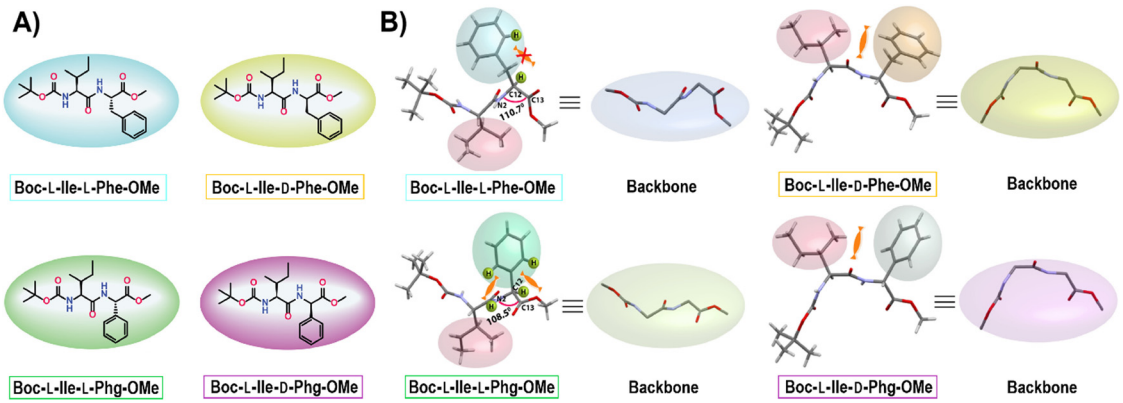

Fig. 13 The X-ray crystal structures of N- and C-protected L/L and D/L dipeptides containing such amino acids as Boc-L-Val-L-Ile-OMe, Boc-D-Val-L-Ile-OMe, Boc-L-Ile-L-Val-OMe, and Boc-L-Ile-D-Val-OMe. Reproduced and adapted from ref. 183 with permission from Elsevier, copyright 2020.

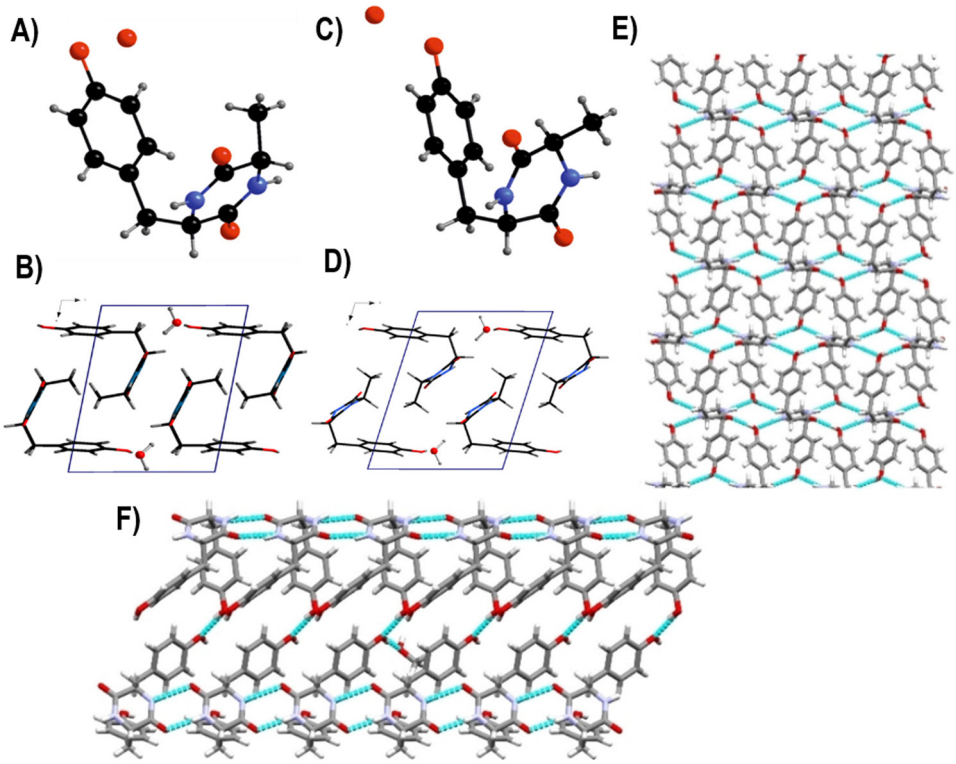

Fig. 14 Molecular and crystal structures for cyclo(L-Tyr-L-Ala) (panels (A) and (B)) and cyclo(L-Tyr-D-Ala) (panels (C) and (D)); (E) hydrogen bonding network present in the crystal structure of cyclo(L-Tyr-L-Tyr) cY(D)Y; (F) hydrogen bonds network observed in the crystal structure of cyclo(L-Tyr-L-Tyr) methanol solvate. Reproduced and adapted from ref. 184 with permission from American Chemical Society, copyright 2015, and from ref. 185 with permission from John Wiley and Sons, copyright 2022.

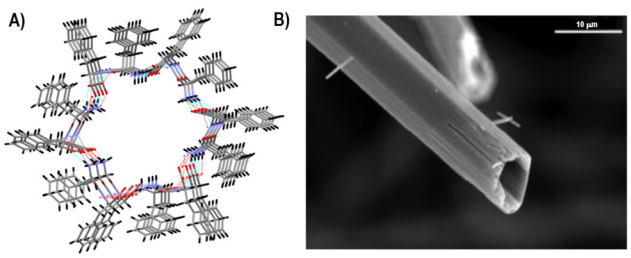

Fig. 15 (A) Supramolecular structure formed by multiplication of chiral structural synthon (CSS) of L-Phe-L-Phe or D-Phe-D-Phe; (B) SEM picture of peptide nanotube (PNT) formed by L-Phe-L-Phe or D-Phe-D-Phe. Reproduced and adapted from ref. 186 with permission from American Chemical Society, copyright 2012.

groups is anti-planar, then there is no chance to form nanotubes. In this case, the peptide nanowires might be formed (see Fig. 16A and B). The influence of solvent type on morphology, assembly kinetics, and orientation of Phe-Phe peptides has been explored both experimentally and computationally, revealing that its lower solvophobicity in methanol results in much weaker self-assembly.[175,187]

The chemically modified di- and tri-peptides offer a great variety of self-assembling structures and thus have been largely studied in recent years, especially for biomedical and material applications.[10,167,188] Recently, it has been discovered that halogenation affects supramolecular organization, in particular, fluorination leads to the preservation of dipeptide packing in the water channels, while iodination completely changes the packing from the water channels to the amphipathic layers of the stacked peptides.[189] Marchesan and coworkers for the analysis of the self-organization of heterochiral and halogenated dipeptides have employed modifications of fluorine or iodide substituted Phe–Phe. In particular, fluorination maintained the arrangement of dipeptides within aqueous channels, similar to what is observed with non-halogenated dipeptides. This modification provided an intermediate level of intra-*versus* inter-molecular hydrophobic interactions, leading to a moderate level of fibril bundling (Fig. 17).[189] SC-XRD structures revealed that despite the different stereo-configurations of homochiral and heterochiral diphenylalanine, they displayed a similar supramolecular packing, although the N-terminal amino acid dictated the screw-sense handedness from N- to C-terminus to be left-handed for L-Phe-L-Phe and right-handed for D-Phe-L-Phe (see Fig. 18). Moreover, the heterochiral peptide displayed an increased intramolecular hydrophobic contact area between Phe side chains.

Of the twenty amino acids known, proline is a very special case due to its unique structure. Unlike most amino acids, proline contains a cyclic side chain in which the nitrogen atom is part of a five-membered ring. The change in conformation and/or puckering of the five-membered ring may be another

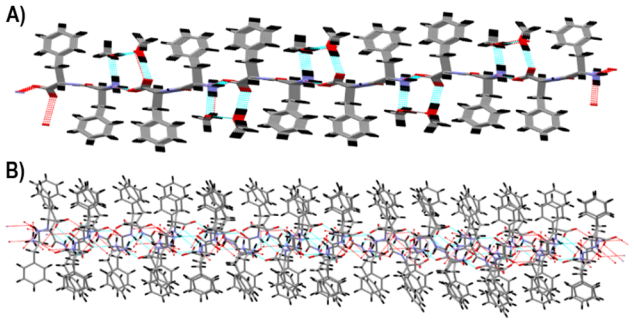

Fig. 16 Supramolecular structure formed by multiplication of chiral structural synthon (A) L-Phe-L-Phe crystallized from methanol; (B) racemic mixture of D-Phe-D-Phe and L-Phe-L-Phe.

factor (in addition to chirality) that can have a strong effect on the self-assembly of short peptides. To explain the role of proline in the formation of functional nanostructures, Garcia *et al.* studied D- and L-amino acids in the Pro-Phe-Phe sequence (see Fig. 19) to resolve the conflict between the contradictory assembly directing effects of Pro as β-breaker and Phe-Phe as a β-sheet-associated motif.[190]

Based on the obtained results, the authors concluded that the stereo-configuration determines the ability of each of the eight possible Pro-Phe-Phe stereoisomers to self-associate into diverse nanostructures, including nanoparticles, nanotapes, or fibrils, which yielded hydrogels with gel-to-sol transition at a physiologically relevant temperature.

Going further with understanding the role of proline chirality in the self-assembly of peptides Chatterjee *et al.* have studied the nature of the conformational preferences of four distinct classes of model diproline peptides, by crystallographic and NMR studies.[191] The analysis of pyrrolidine conformations suggested a preferred proline puckering geometry favored only in the case of heterochiral diproline segments. Moreover, a detailed view of the possible conformational states of heterochiral and homochiral Pro-Pro sequences was additionally supported by the NMR studies in solution. Of the fourteen systems studied, the crystal and molecular structures of the two heterochiral tripeptides Piv-L-Pro-D-Pro-L-Ala-OMe and Piv-D-Pro-L-Pro-D-Ala-OMe were also discussed. The first system crystallizes in $P2_12_12_1$ (19) space group and $Z' = 1$ (Fig. 20A) while the second one in $P2_1$ (4) space group and two independent molecules in the crystal lattice ($Z' = 2$) (Fig. 20B and C).

The molecular structure of each molecule displayed in Fig. 20 shows subtle differences in the conformation of the proline ring. On the other hand, the D-Pro-Pro motif is known to serve as an inducing element of β-torsion, while homochiral Pro-Pro induces local helical folding.[192,193] The localization of D-Pro in the peptide sequence may also be an important factor in determining supramolecular organization. Fig. 21 shows the supramolecular structure for Piv-L-Pro-D-Pro-L-Ala-OMe and Piv-D-Pro-L-Pro-D-Ala-OMe tripeptides. A strong tendency to form fibers is evident in the second case.

It is interesting to note that even single aromatic amino acids can self-assemble into amyloid-like fibers. Specifically, phenylalanine (Phe) and tryptophan (Trp) were found to be important in nanostructure formation in many different studies.[194–197] Recently, Bera *et al.* decided to explore the effect of D-enantiomers of these amino acids on the self-assembly pattern and the molecular arrangement of the resultant structural organization and demonstrated the critical role of chirality in the process. The authors applied a wide range of different experimental techniques to probe the self-assembly

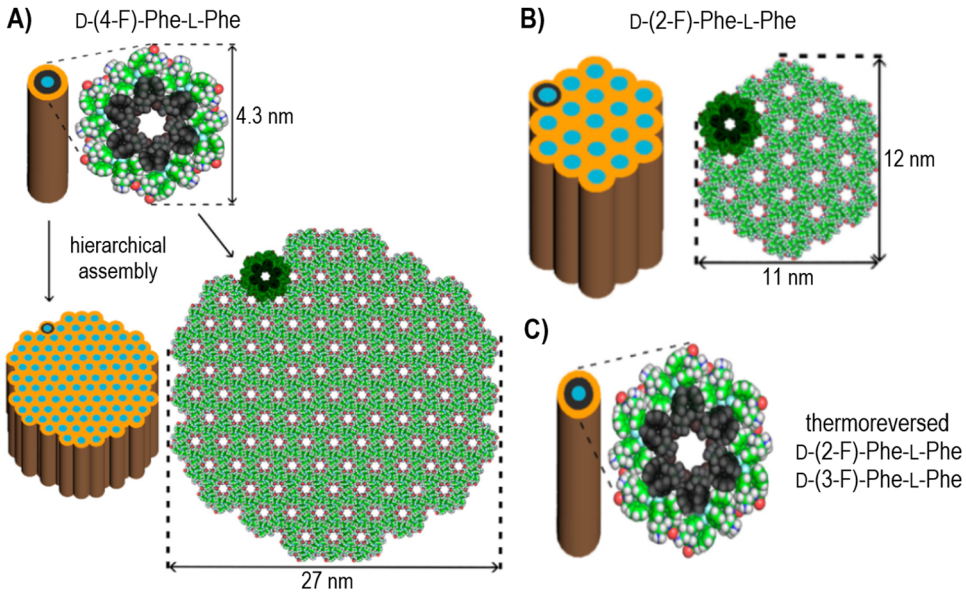

Fig. 17 (A) Single-crystal XRD structure (CCDC 2016373) of D-(4-F)-Phe-L-Phe; (B) and (C) powder XRD on microcrystals grown on hydrogels of D-(2-F)-Phe-L-Phe and D-(3-F)-Phe-L-Phe confirmed packing analogous to sample D-(4-F)-Phe-L-Phe. Reproduced and adapted from ref. 189 under the terms of the Creative Commons CC BY 4.0 license (https://creativecommons.org/licenses/by/4.0).

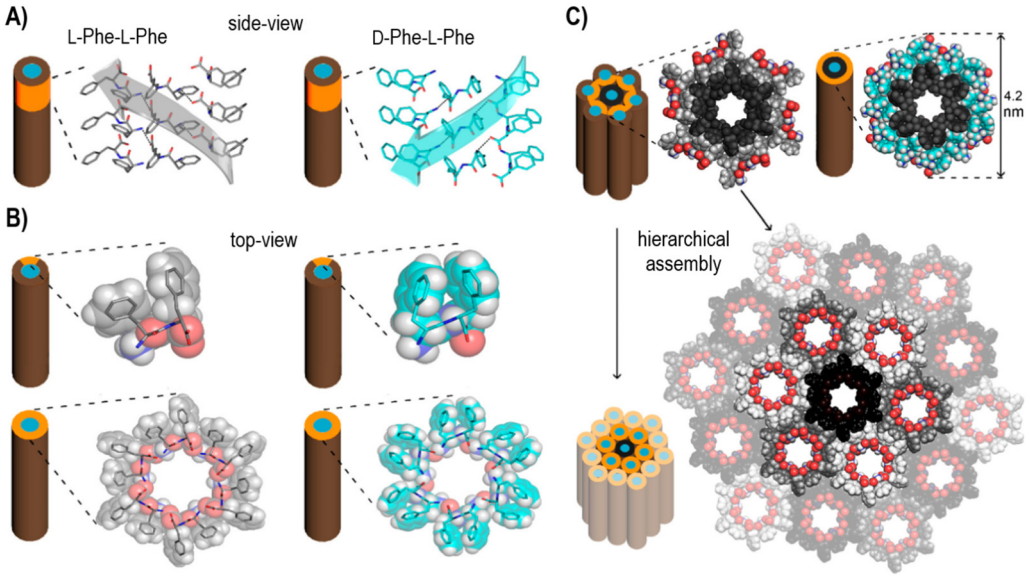

Fig. 18 Single-crystal XRD structures of homochiral L-Phe-L-Phe[36] (silver) and heterochiral D-Phe-L-Phe (cyan, CCDC 2016375) peptide nanotubes.[37] (A) Side-view of homochiral and heterochiral peptides revealed opposite screw-sense, dictated by the N-terminal amino acids. (B) Top-view of nanotube inner cavities defined by the projection six peptide molecules arranged head-to-tail. (C) Top-view of the nanotubes identified by the projection of 18 peptide molecules showing hierarchical bundling stabilized by aromatic zippers for L-Phe-L-Phe (silver) and a smoother outer surface, with an outer diameter matching well the fibril size in a case of D-Phe-L-Phe (cyan). Reproduced and adapted from ref. 189 under the terms of the Creative Commons CC BY 4.0 license (https://creativecommons.org/licenses/by/4.0).

mechanism and the involvement of various interactions in the structure formation. The DL-composites of aromatic amino acids have a high aggregation propensity and present a favorable knob-to-hole packing of aromatic rings, which induced the easy growth of racemic crystals and the fabrication of self-assembled rigid materials (see Fig. 22).[198] The potential of D- and L-enantiomers of phenylalanine was later further explored towards the development of functional metal–organic materials.[199,200] Taking into account the association of some self-assembling peptides with pathological conditions, such as the amyloid-β in Alzheimer's disease, there is a tremendous interest in studying the short amyloidogenic sequences.

The influence of stereochemistry on self-organization in the solid state of cyclic dipeptides (CDP) employing two diastereomeric samples; cyclo(L-Tyr-L-Ala) and cyclo(L-Tyr-D-Ala) as models was investigated by Jeziorna *et al.*[184,186] It has been found that distinction in chirality of alanine residue causes a significant difference in self-assembling and formation of higher order structures. Sample cyclo(L-Tyr-L-Ala) forms peptide nanotubes (PNT) and nanowires (PNW) (see Fig. 23A and B), while for sample cyclo(L-Tyr-D-Ala) only formation of peptide microtubes (PMT) was observed (see Fig. 23C and D). Crystal and molecular structures for both samples were refined using PXRD due to failure in attempts to grow crystals with quality suitable for single crystal studies. Both compounds crystallize in the $P2_1$ space group and monoclinic system. The size of the unit cell is highly similar; however, small differences in alignment of water molecules in the hydrophilic channels and geometry of diketopiperazine rings were observed. The water molecules can be thermally removed from the lattice without destroying the subtle crystal structures of nano- and microdevices. This reversible process observed for cyclo(L-Tyr-D-Ala) is a unique feature, rarely occurring for the linear dipeptide devices.

Finally, it is worthy to stress that the self-organization of heterochiral peptides can be controlled by chemical modification of the protecting group. For example, peptides related to the Ala-Ala building block have been investigated by Lin *et al.*[201] In their work, a special focus has been given to the position of the substituent attached to the benzoyl residue at the N-terminus, on the molecular packing, and the self-assembly behavior. Specifically, three peptide isomers with an *ortho*-, *meta*-, and *para*-dodecyloxy group on the benzoyl residue at the N-terminus were designed and synthesized (see Fig. 24). It was demonstrated that the *ortho*- substituent position presents a strong steric hindrance and the occurrence of intramolecular hydrogen bonding, resulting in different molecular packing compared with the two other isomers.

5. Formation of gels

Many self-assembling peptides can create new functional soft matter, such as hydrogels or organogels. Hydrogels are characterized by a high amount of water inside the network, making them biocompatible and biodegradable, thus making them auspicious materials for biological and biomedical applications. On the other hand, organogels are created by the entrapment of large amounts of organic solvents into the peptide assemblies. Peptide-based gels are stimuli-responsive

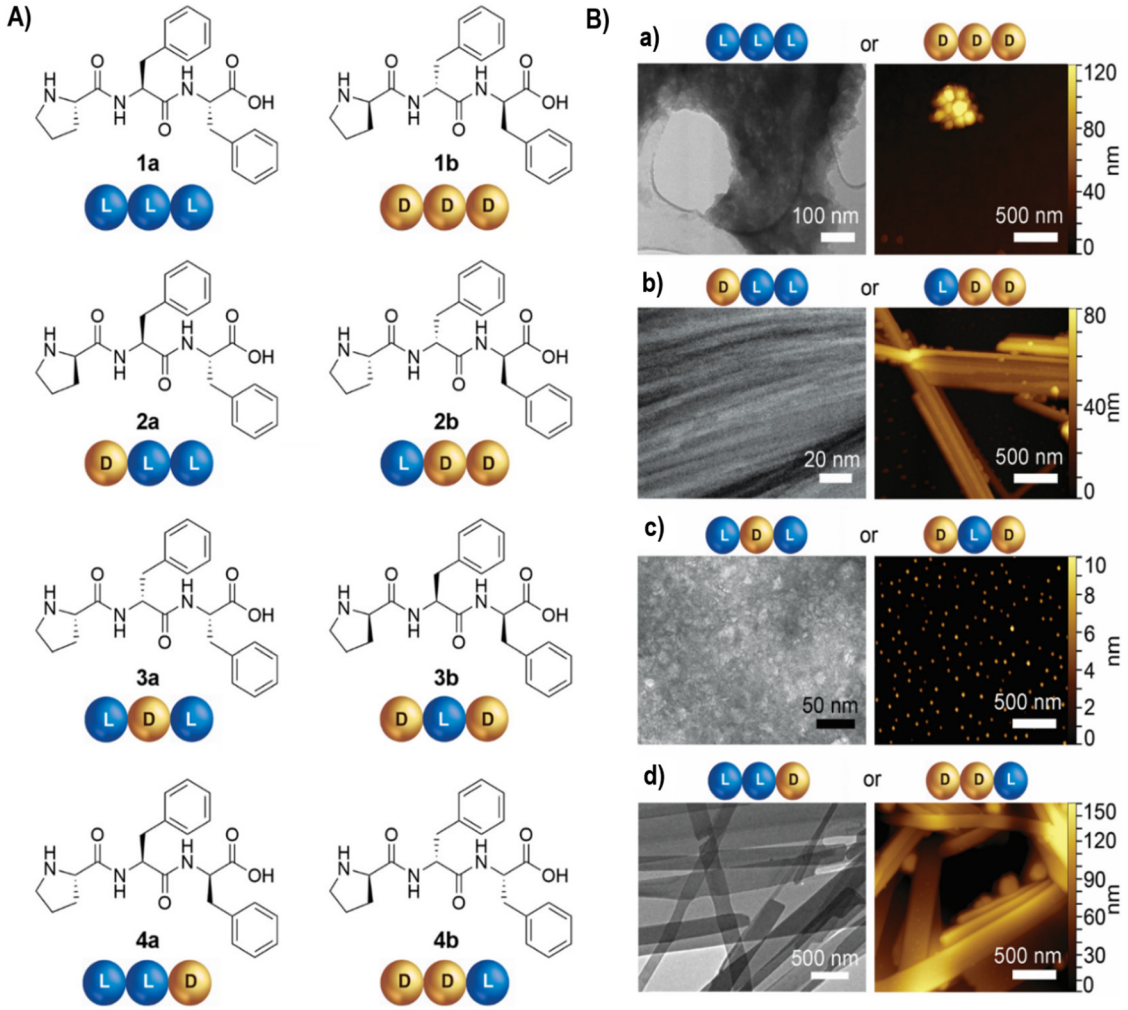

Fig. 19 (A) Pro-Phe-Phe Stereoisomers by Enantiomer Pairs (a/b) and Their Cartoon Keycode (Each Amino Acid is Represented as Either a Blue (L) or Gold (D) Sphere); (B) TEM (left) and AFM (right) images: (a) **1a** aggregates, **2a** bundles of nanofibrils, (c) **3a** nanoparticles, (d) **4a** nanotapes. Reproduced and adapted from ref. 190 under CC BY 4.0 license (https://creativecommons.org/licenses/by/4.0).

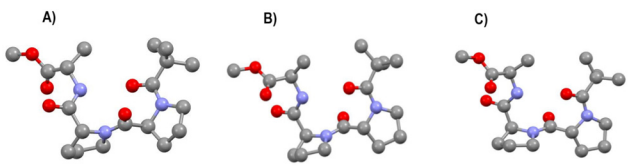

Fig. 20 Molecular structure of tripeptides: (A) Piv-L-Pro-D-Pro-L-Ala-OMe; (B) and (C) Piv-D-Pro-L-Pro-D-Ala-OMe.

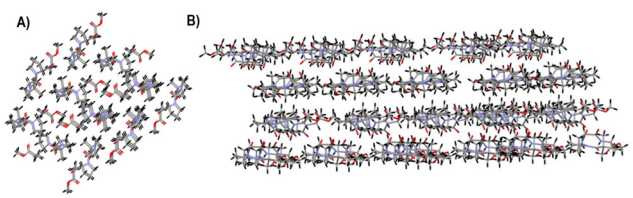

Fig. 21 Supramolecular structure formed by multiplication of chiral structural synthon (CSS): (A) Piv-L-Pro-D-Pro-L-Ala-OMe and (B) Piv-D-Pro-L-Pro-D-Ala-OMe.

and sensitive to the type of solvent, presence of salts, pH, temperature, or ultrasounds, thus, they can be easily affected by environmental chemical and physical stimuli. Many other internal factors, including chirality, influence the gelation properties of peptides and might be used as a valuable tool for driving self-assembly. Effects observed at molecular and supramolecular levels, described in detail in the previous chapters, are amplified through increasing size scale to macroscopic changes and finally affect the properties of peptide-based materials.

The influence of molecular packing and structural features on the properties of peptide-based hydrogels has been extensively studied, offering valuable insights into their design. Chirality effects play a crucial role in the self-assembly and macroscopic properties of peptide hydrogels. A great number of insights into the effects of chirality on peptide-based soft matter have been delivered in works published by Marchesan and co-workers. Studies on dipeptides like Phe-Val and Val-Phe

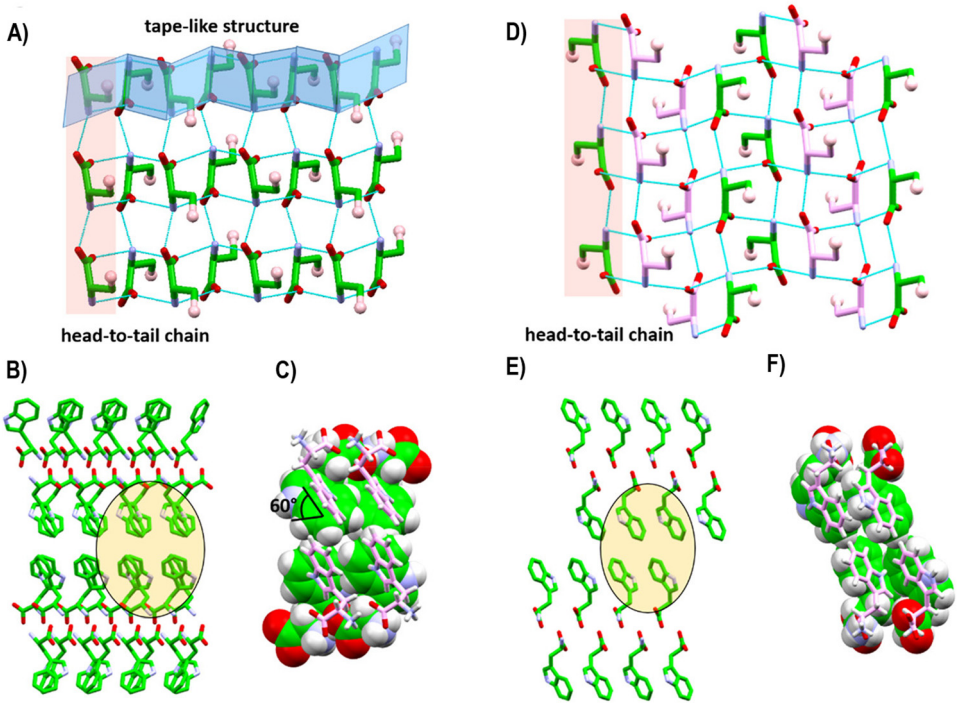

Fig. 22 Single-crystal structural analysis of (A)–(C) L-Trp and (D)–(F) DL-Trp. L-Trp: (A) molecular chain formation (pink) and tape-like arrangement (blue); (B) supramolecular β-sheet structure; (C) twisted angle between two adjacent aromatic rings highlighted by a yellow circle in (B). DL-Trp: (D) 3D network arrangement through H-bonding interactions of molecular chains (pink); (E) supramolecular β-sheet structure; (F)"Knobs-in-holes" fitting of adjacent aromatic rings highlighted by a yellow circle in (E). Reproduced and adapted from ref. 198 under CC BY 4.0 license (https://creativecommons.org/licenses/by/4.0).

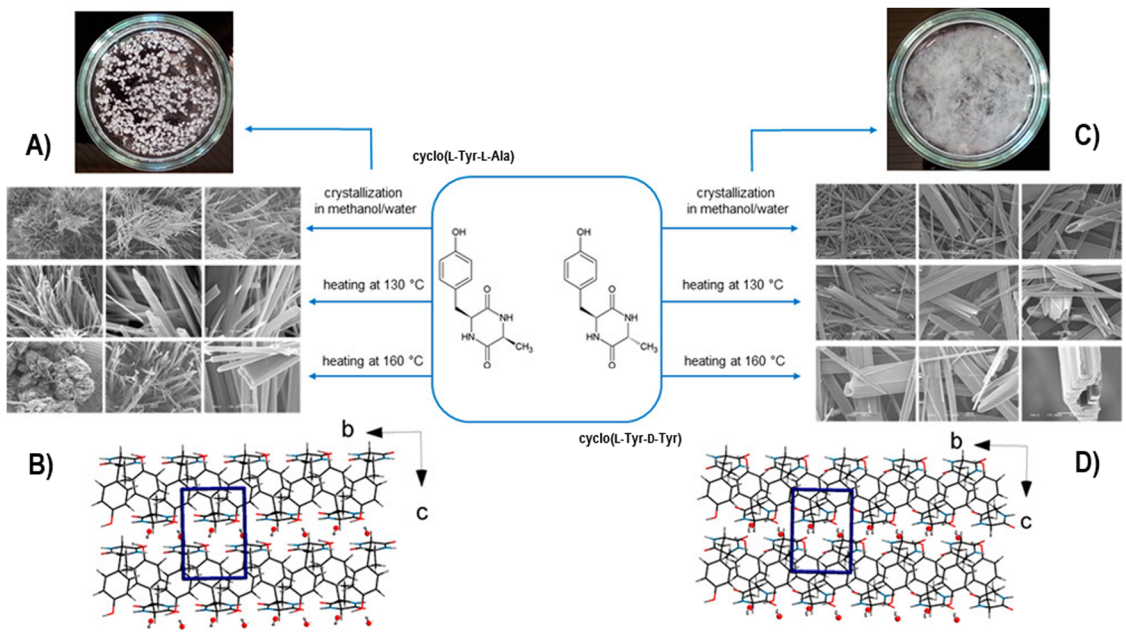

Fig. 23 SEM images of cyclo(L-Tyr-L-Ala) (A) and cyclo(L-Tyr-D-Ala) (C); supramolecular array of cyclo(L-Tyr-L-Ala) (B) and cyclo(L-Tyr-D-Ala) (D). Reproduced and adapted from ref. 184 with permission from American Chemical Society, copyright 2015.

demonstrated that heterochirality enables fibrillation and gelation from otherwise non-gelling homochiral sequences (see Fig. 25).[202]

Likewise, the four stereoisomers of Leu-Phe dipeptides revealed that heterochirality promotes hydrogelation, with all heterochiral dipeptides forming stable gels and one specific

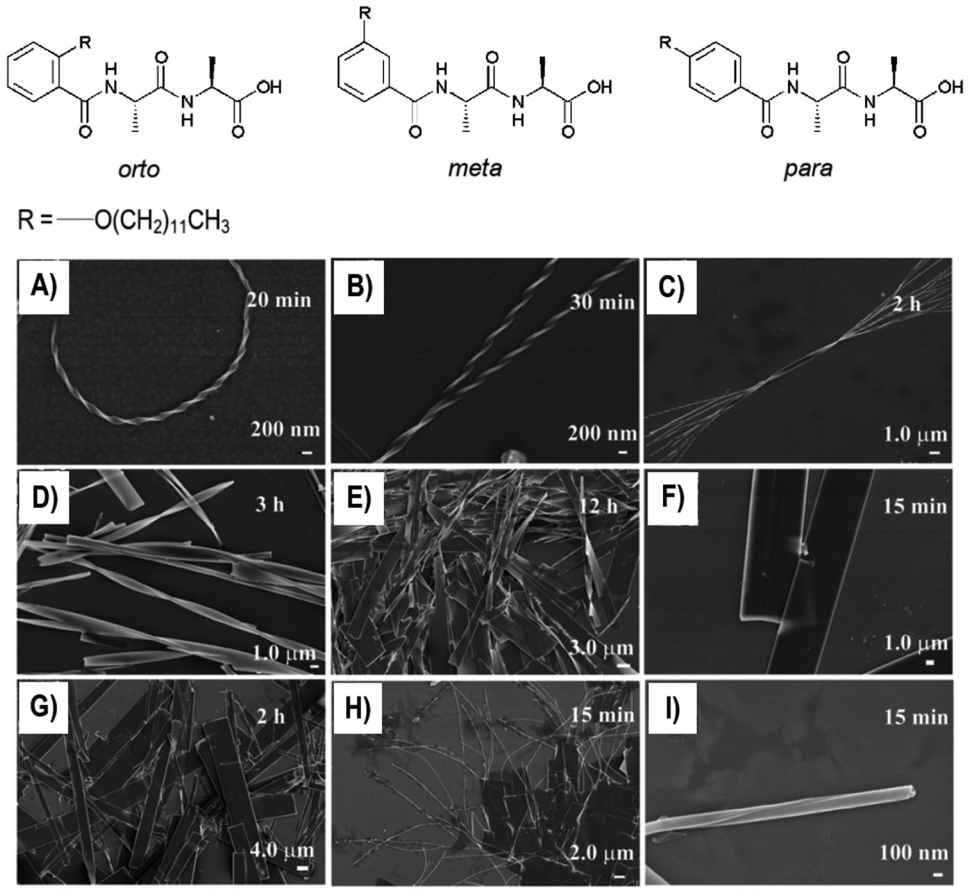

Fig. 24 FE-SEM images of the three dipeptide self-assemblies. All samples were prepared in a CH_3OH/H_2O mixed solvent (6/4, v/v) at a concentration of 2.0 g L^{-1}; *ortho* (A)–(E), *meta* (F) and (G) and para (H) and (I). Reproduced and adapted from ref. 201 with permission from Royal Society of Chemistry, copyright 2021.

configuration (D-Phe-L-Leu) leading to metastable hydrogel converting into crystals.[203] Investigations of tripeptides, such as Val-Phe-Phe and Phe-Phe-Val, highlighted the influence of D- and L-amino acid positions on supramolecular order and macroscopic properties. For instance, configurations like DLL or LDD facilitated the formation of hydrophobic channels that excluded water, resulting in durable hydrogels with high thermal stability. Conversely, other configurations formed lower-order assemblies, leading to weaker gels.[204]

Steric hindrance is another important factor in hydrogel formation and stability. For example, investigations into tripeptides such as D-Leu-L-Phe-L-Phe revealed that heterochirality promotes hydrogelation in an aqueous solution following a pH switch through extended 3D molecular structures. This arrangement supports the formation of elongated fibers, high fiber density, and large fiber bundles, resulting in immediate macroscopic gelation. In addition, a phenylalanine zipper has been identified as an important interaction motif between interdigitated β-sheets of the D-Leu-L-Phe-L-Phe. In contrast, the sterically hindered L-epimer did not gel, highlighting the significance of steric considerations.[205] Similarly, studies showed that peptides with β-branched amino acids (such as valine or isoleucine) formed dense networks with higher resistance to applied stress, while in contrast the linear side chains negatively affected hydrogel durability and rheological properties.[206]

Also, the high supramolecular order was shown to significantly influence the mechanical and thermal properties of peptide-based hydrogels. The presence of tightly packed β-sheets and hydrophobic channels contributed to enhanced gel durability. Notably, stereoisomers such as D-Val-L-Phe-L-Phe and L-Val-D-Phe-D-Phe exhibited contrasting behaviors in water exclusion and stability, which were directly linked to their ability to form high-order supramolecular structures. Specifically, in the mentioned configuration the dry hydrophobic channels are formed, resulting in the exclusion of water molecules, giving rise to a higher supramolecular order.[207] In case of some tri-peptides, the formation of a racemic mixture can lead to novel or improved properties of the gel. It has been described that the co-assembly of tripeptides: L-His-D-Phe-D-Phe and D-His-L-Phe-L-Phe forms anisotropic nanostructures that form gel with better viscoelastic properties and enhanced catalytic activity.[208]

Finally, the influence of external stimuli, such as ultrasound, was studied to optimize nanostructure alignment towards anisotropic organo- and hydrogels consisting of oriented tripeptide

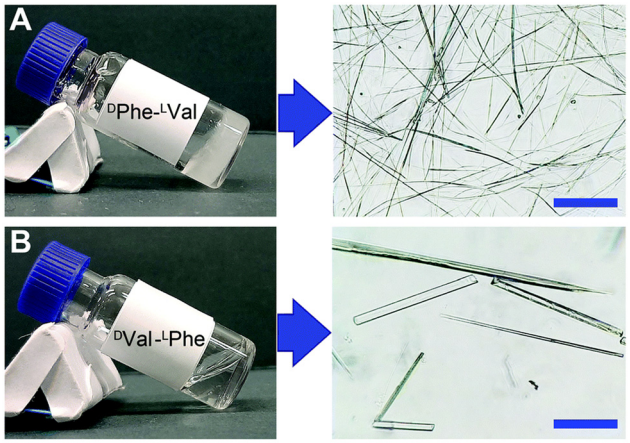

Fig. 25 Photographs and optical microscopy images of (A) D-Phe–L-Val and (B) D-Val–L-Phe in PBS at concentrations above their solubility. Scale bar = 100 μm. Reproduced and adapted from ref. 202 with permission from Royal Society of Chemistry, copyright 2022.

structures based on D-Phe-L-Phe-L-Asp and D-Phe-L-Phe-L-Ile. The former peptide formed an anisotropic organogel in methanol, while the latter formed an anisotropic hydrogel, showing the relationship between the anisotropic arrangement of supramolecular interactions with peptide sequence and solvent environment.[209]

In addition to frequently studied linear peptides, the gelling properties of their cyclic analogues are sporadically explored. It was found that while cyclo(L-Tyr-L-Tyr) easily assembles into hydrogels, conformation of cyclo(D-Tyr-L-Tyr) promotes rather two-directional growth, resulting in a tendency towards crystallization.[185] Interestingly, heterochiral cyclodipeptides cyclo(D-Leu-L-Phe) and cyclo(L-Leu-D-Phe) are able to form gels in a soybean oil.[210]

5.1. Heterochirality in biomedical approaches

In many cases, biological applications and biocompatibility of the peptide-based materials are explored alongside structural insights. Especially, since peptides containing D-amino acids are considered a great tool in biomedical research due to their resistance to enzymatic degradation. Since human proteases exclusively recognize and cleave L-amino acids, replacing them with their D-enantiomers makes peptides more resistant to proteolysis, significantly increasing their biostability. Consequently, the improved stability may translate into better *in vivo* circulation half-lives, improving delivery yield and efficacy, and potentially reducing dosing frequency.

Many naturally occurring antibiotics, such as dactinomycin, bacitracin, gramicidin, and others, contain D-amino acid residues in their sequences. In many cases, the pattern formed by the alternation of D- and L-amino acids is crucial for the formation of the peptide's proper structure, with gramicidin helices being one of the most important examples.[211] Thus, a lot of scientific attention in organic chemistry has been given to the total synthesis of peptide antibiotics, highlighting the role of heterochirality in their structural and functional properties.[212] Over the years, heterochiral peptides have been used not only as antimicrobial agents.[213,214] but also as potential cancer therapeutics[215,216] and vaccine candidates.[217] The recent progress and challenges in the exploration of D-amino acids at the interface of chemistry and life science have been nicely reviewed elsewhere,[218,219] as well as their role in antimicrobial resistance,[220,221] and in numerous physiological processes in the human body.[222–224] Therefore, in this chapter, we would like to briefly introduce some recent examples focusing specifically on the biomedical applications of hydrogels based on heterochiral peptides.

Most of the gelling peptides, regardless of chirality, demonstrated excellent performance in cell culture experiments, with no significant differences observed between enantiomers in supporting cell viability and proliferation. For example, both D-Val-L-Phe-L-Phe and L-Val-D-Phe-D-Phe gelling peptides performed well in cell culture experiments, with no cytotoxicity observed.[207] Such results support the potential future development of cost-effective biomaterial gels from heterochiral assembling peptides. One of the envisioned biomedical applications of peptide hydrogels is their possible role as cell scaffolds. Unfortunately, the native amino acids can be easily decomposed by proteolytic enzymes, making them mostly unsuitable for this application. Thus, sequences containing D-amino acids might offer a reasonable alternative. For instance, a hydrogel formed by a D-P1 peptide (Ac–Phe–Phe–Phe–Gly–Lys) has gelation properties like its L-form,[225] but is resistant to a protease, stable in a cell-culture medium, and can serve as a scaffold for cell cultures.[226] Few relevant studies on other peptide sequences explored further different aspects of chirality influence the hydrogel properties and degradation, as well as its impact in biological context, especially towards novel immunotherapies.[227–229] Co-assembly and stereocomplexation are promising strategies for improved rigidity and generation of hybrid biomaterials, applicable, for example, in regenerative medicine.[230–232] They can dramatically affect hydrogel stiffness and degradation, allowing control over novel shapes, network morphologies, and material properties, and offer proteolytic stability for the material's lifetime control.

Much less is known about the gelation process in longer peptides, and especially how it is affected by the changes in chirality. One interesting recent example describes a systematic D-scan of natural hexapeptide Phe-Ile-Asn-Tyr-Val-Lys that was performed, including the biophysical characterization of the obtained hydrogels and their biocompatibility. Despite the differences in the conformational intermediates during aggregation, all sequences resulted in hydrogels compatible with a cellular environment.[233]

6. Self-assembly and gel formation with chemically modified heterochiral peptides

In recent years, many groups have focused their research not only on the native peptide sequences but also on modified

peptides and peptide-based conjugates, expanding the scope of native peptide studies to explore new ways of influencing self-assembly processes. This concept is based on the idea that the gelling properties of peptides can be affected by both chirality and the presence of chemical modifications. Even the mere presence of molecular chirality in a peptide sequence has a crucial impact on its supramolecular assembly and gelation, as has been shown for 1,8-naphthalimide (NMI)-conjugated hybrid dipeptides. While chiral NMI derivatives (NMI-βAla-L-Val-OMe and NMI-βAla-D-Val-OMe) formed self-supported gels, the achiral NMI derivative (NMI-βAla-Aib-OMe) failed to form any kind of gel.[234] In many examples, peptide gelators were believed to require a single enantiomer for gelation, however, some recent studies demonstrate that heterochiral sequences can yield gels with unique properties. McAulay *et al.* explored the dipeptide 2Nap-Phe-Phe containing naphthyl (Nap) group, which is a popular building block for assisting peptide self-assembly, developing immune adjuvants, and adding specific electrical properties. In their investigations, all enantiomers, diastereomers, and even racemates of this dipeptide could form gels at high pH.[235] These findings were further supported by a cryo-EM near-atomic resolution approach. The pH-dependent gelation mechanism has been explained by the tubes' carbonyl group protonation that allows them to come together and form a gel.[236]

The possibility of gelation in racemic mixtures was also explored in the case of modified cyclic dipeptides – specifically fluorenyl (OFm) mono-substituted cyclo(L-Glu-L-Glu). Their racemate enables gelation in a large variety of organic solvents and water and displays a tunable thixotropic behavior.[237] This ability of peptide racemates to gel broadens the design possibilities for novel gel-based materials.

The effects of subtle changes in chirality can significantly influence biofunctionality and mechanical properties, for instance as described for Nap-containing peptides. Specifically, Nap-L-Gly-L-Phe-L-Phe-L-Tyr, have been used to create vaccine adjuvant hydrogels.[228] Its heterochiral variant, Nap-L-Gly-L-Phe-L-Phe-D-Tyr, showed improved mechanical properties and resistance to external forces, due to their dense nanofiber network (see Fig. 26).[238]

Ferrocene (Fc)-based peptide conjugates offer another example of modified systems with tunable self-assembly and gelation behaviors, especially due to the interesting structural properties of the Fc group. Studies on monosubstituted Fc conjugates (FcCO–Phe-Phe-Ala-OMe) demonstrated the dramatic effects of diastereomeric interactions on gelation, with enantiomers showing no significant impact.[239] A ferrocene-diphenylalanine (Fc-Phe-Phe) peptide derivative forms stable chiral nanostructures in a narrow pH range (5.7–5.9) (Fig. 27). Compared to the uniformly chiral Fc-L-Phe-L-Phe, a racemic mixture of the L and D enantiomers resulted in formation of weaker and less stable gels, demonstrating the crucial role of molecular chirality.[240]

The impact of chirality on modulation of photoresponsive behaviors was analyzed in a case of azobenzene-modified dipeptides. Chiral gelators have been built on LL-dipeptides or DD-dipeptides with an azobenzene group functioning as a bridge between the peptide units. These gelators, built on LL- or DD-dipeptides demonstrated distinct gel–sol transition speeds during the *trans*-to-*cis* (*E*/*Z*) isomerization of the azobenzene group.[241] The self-assembly of azobenzene-linked chiral dipeptide gelators can also be modulated by circularly polarized light (CPL). In such case right-handed CPL causes the gel to collapse, whereas left-handed CPL promotes new

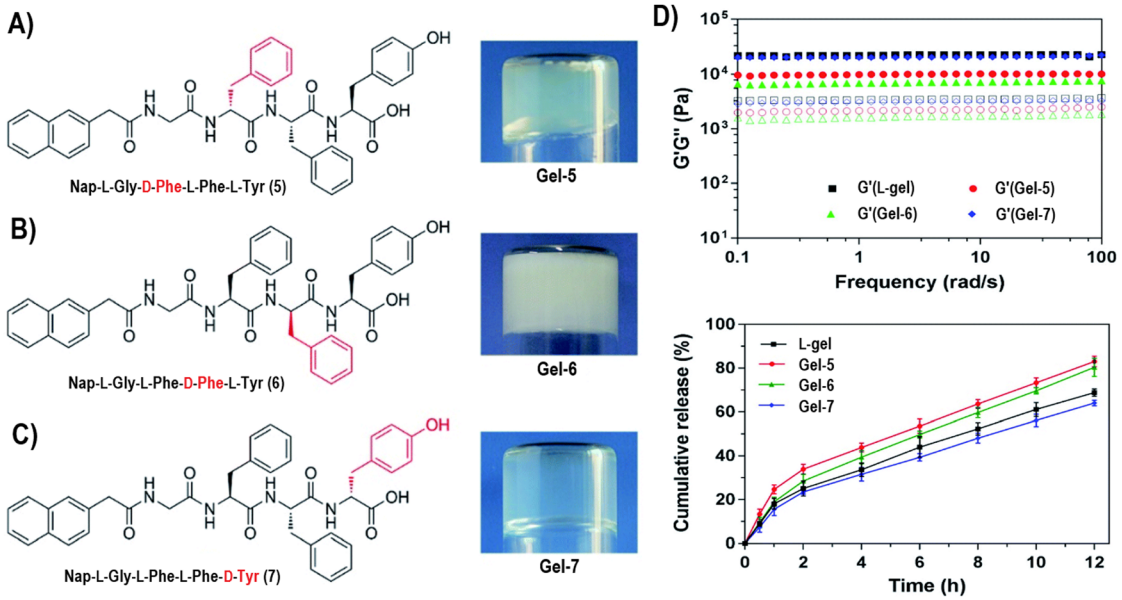

Fig. 26 The chemical structures and optical images of (A) Nap-L-Gly-D-Phe-L-Phe-L-Tyr (**5**) (B) Nap-L-Gly-L-Phe-D-Phe-L-Tyr (**6**), and (C) Nap-L-Gly-L-Phe-L-Phe-D-Tyr (**7**) hydrogels and their mechanical properties (D). Reproduced and adapted from ref. 238 under the terms of the Creative Commons CC BY-NC 3.0 license.

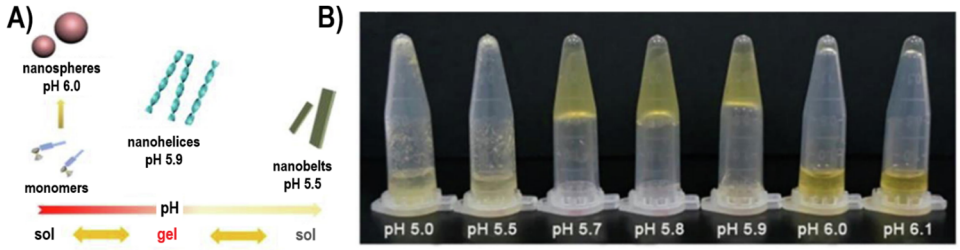

Fig. 27 Schematic illustration for the ultra-pH-sensitive of Fc-L-Phe-L-Phe hydrogel (A) and photographic images showing the self-assembly behavior of 2 mg mL^{-1} Fc-L-Phe-L-Phe in 10% 2-propanol/90% H_2O at phosphate buffer (0.1 M) with different pH values (B). Reproduced and adapted from ref. 240 with permission from Elsevier, copyright 2020.

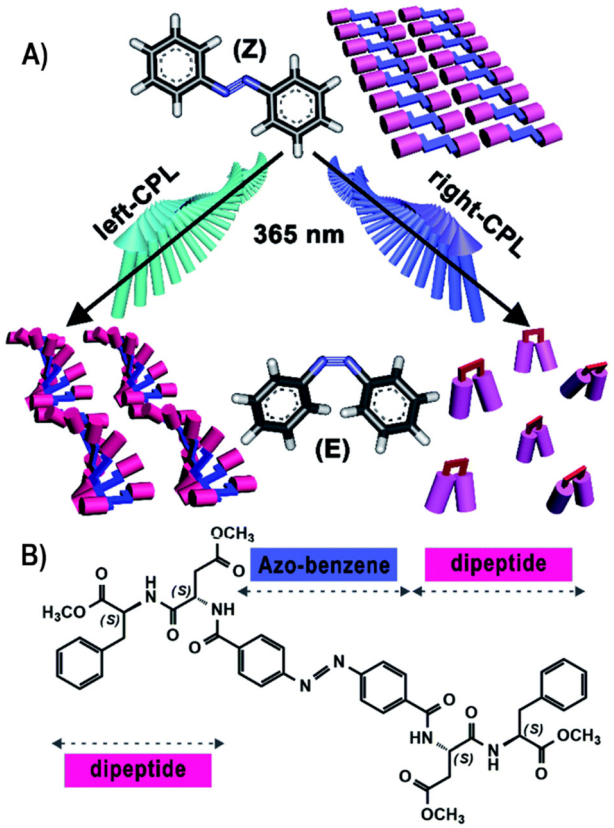

Fig. 28 (A) Illustration of different supramolecular self-assembly modulated by CPL handedness, right-CPL promotes the collapse of ordered structure, but left-CPL triggers the formation of new helical structure; (B) chemical structure of 4,4′-azobenzene-linked dipeptide gelator, abbreviated to Azo-DF. Reproduced and adapted from ref. 242 under the terms of the Creative Commons CC BY-NC 3.0 license.

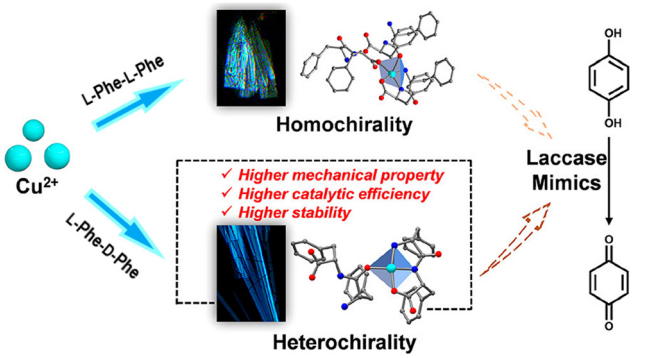

Fig. 29 Schematic illustration of the chirality-dependent coordination assembly process between Phe-Phe molecules and Cu^{2+}, in which the peptide heterochirality leads to enhanced properties of a laccase mimic. Reproduced and adapted from ref. 245 with permission from American Chemical Society, copyright 2022.

self-assembly, maintaining the macroscopic gel structure (see Fig. 28).[242]

Chirality has also been explored in metal-peptide assemblies, where it influences both structure and function. These effect have been understood more deeply in studies focused on single amino acid residues[243,244] but still quite little is known about the effect of chirality on the architectures and properties of metal-peptide assemblies. Zhang *et al.* investigated Phe-Phe dipeptides coordinated with Cu^{2+} ions, forming a metalloenzyme mimic (see Fig. 29). Both the homochiral L-Phe-L-Phe-Cu and their racemate (L/D) Phe-Phe-Cu assemblies demonstrated laccase-like catalytic activity, but the heterochiral assemblies exhibited significantly higher catalytic efficiency and reusability. These results highlight the potential of chirality in tuning the physicochemical properties of functional materials.[245]

Peptide gels also serve as effective media for protein crystallization, with their inherent chirality significantly influencing the process. Conejero-Muriel *et al.* examined the influence of the chirality of the gel fibers in protein crystallogenesis. Two cysteine-based peptides – *N*,*N*′-di(benzoyl)-L-cysteine diamide and its corresponding D-enantiomer have been employed to grow protein crystals, and differences in crystal quality and packing have been observed, suggesting a significant influence of the chirality in this process.[246] Protein crystallization in gels based on the Fmoc-dipeptides family resulted in formation of high-quality protein crystals with enantiomeric hydrogels influencing mostly the nucleation and growth of the same protein.[247]

Amino acid chirality was also employed in the formation of chiral gelators for the self-assembly driven enantioselective recognition. The development of chiral supramolecular gels for enantioselective recognition through gel formation or collapse has been nicely summarized in a review by Gambhir *et al.*[248] Some most notable recent examples involving amino acids, peptides, or their derivatives have been applied to

enantioselective recognition of carboxylates,[249] chiral recognition of mandelic acid and *N*-tosyl α-amino acids,[250] or enantioselective gelation of tartaric acid enantiomers.[251] Future investigations are likely to explore more in-depth the effects of chirality on chiral recognition in other peptide sequences, towards their sensing applications.

7. Conclusion and future perspectives

In recent years, remarkable progress has been made in the field of peptide self-assembly, including studies on the heterochiral peptide systems that combine both L- and D-amino acids. These advanced biomaterials offer unique structural and functional properties that homochiral systems cannot achieve. In this tutorial review, we show analytical tools that allow us to distinguish stereoisomers, describe the problem of chirality and its impact on the organization of higher-order structures, and understand at the molecular level the mechanism of self-assembly and the formation of different hetero-chiral materials with tailored functions. Existing literature highlights chirality as one of the vital factors that can easily and profoundly influence the formation of various peptide morphologies. We believe that one of the most important achievements in the field will be the ability to successfully predict and dictate the formation of heterochiral supramolecular structures. Firstly, it may provide important insights for protein aggregation disorders and subsequently lead to the discovery of amyloid formation inhibitors and new therapeutic approaches. Secondly, it will offer the possibility to create novel soft materials with pre-designed properties for various applications in biomedicine, catalysis, nanotechnology, *etc.* Finally, it will broaden our basic understanding of self-organization significantly, improving our knowledge about one of the fundamental bases for the bottom-up creation of artificial life-like systems. Even though a lot of progress has been made in recent years, it remains challenging to draw a pattern allowing for a straightforward prediction of the chirality switching influence on the self-assembly of a particular peptide. The current progress in machine learning (ML) and deep learning (DL) approaches will inevitably result in a more rationalized design of heterochiral peptide sequences with predictable properties.

The spectrum of future applications is vast, demanding, and far from routine solutions. The structure of this review and the choice of the presented material reflect our belief that overcoming these challenges will require investigations combining a wide range of novel experimental and computational methods, often including hybrid techniques. A lot of progress is anticipated especially in studies of peptide assembly dynamics, with the use of the latest techniques, such as advanced microscopic imaging *via* fluorescence lifetime imaging microscopy (FLIM), single-molecule fluorescence lifetime correlation spectroscopy (FLCS),[252] stochastic optical reconstruction microscopy (STORM),[253] and others, that might be particularly interesting in studies of self-assembly. Further improvements are also expected from state-of-the-art spectroscopic methods, such as time-resolved synchrotron radiation circular dichroism (tr-SRCD),[254] surface-enhanced Raman spectroscopy (SERS),[255] new NMR approaches,[256] and many more. Undoubtedly, such a cutting-edge approach will require interdisciplinary collaboration across chemistry, materials science, biology, and engineering.

Finally, based on current research trends and technological advancements, several exciting prospects are emerging for biomedical functional materials formed by the self-assembly of heterochiral peptides. Future bio-applications include work to improve the mechanical properties of peptide gels through topological control, as well as advanced antimicrobial and therapeutic applications, personalized medicine, and targeted drug delivery systems. Additionally, advances in the development of biomimetic materials and tissue engineering are anticipated. However, since the incorporation of D-amino acids has significant biological importance, altering stability, solubility, cytotoxicity, assembly, and therapeutic effects, biological studies must explore deeper cell interactions with peptides of altered chirality, their bioavailability, and biodegradability. Moreover, manufacturing heterochiral peptide compounds presents additional challenges, related to the complex synthesis, scalability, high costs, and difficulties with purification and analysis. The regulatory concerns and GMP considerations must also be addressed to enable the successful production of such materials for clinical use.

In summary, to realize the full potential of D-amino acid-containing peptides as self-assembling materials, future research must incorporate interdisciplinary strategies that combine advanced characterization techniques with AI-driven design. At the same time, deeper biological investigations will be crucial for safe and effective biomedical applications, towards clinical use. Based on the remarkable advancement in recent years, we expect to observe even faster progress in the field soon, with great promise in the use of engineered heterochiral peptides as a versatile and functional platform for next-generation therapies and technologies.

Conflicts of interest

There are no conflicts to declare.

Data availability

No primary research results, software or code have been included and no new data were generated or analysed as part of this review.

Acknowledgements

This work was supported by a Polish National Science Centre (NCN) [Grant No. UMO-2022/47/I/ST4/01629].

References

1 L. D. Barron, *Chem. Soc. Rev.*, 1986, **15**, 189–223.
2 L. D. Barron, *Space Sci. Rev.*, 2008, **135**, 187–201.

3 *Stereochemistry. A Three-Dimensional Insight*, ed. A. V. Karnik and M. Hasan, Elsevier, 2021.
4 Q. Sallembien, L. Bouteiller, J. Crassous and M. Raynal, *Chem. Soc. Rev.*, 2022, **51**, 3436–3476.
5 V. A. Pavlov and E. I. Klabunovskii, *Curr. Org. Chem.*, 2014, **18**, 93–114.
6 J.-M. Cavaillon and S. Legout, *Biomolecules*, 2022, **12**, 596.
7 H. D. Flack, *Acta Crystallogr., Sect. A:Found. Crystallogr.*, 2009, **65**, 371–389.
8 A. B. Buda, T. A. der Heyde and K. Mislow, *Angew. Chem., Int. Ed. Engl.*, 1992, **31**, 989–1007.
9 J. Wang, K. Liu, R. Xing and X. Yan, *Chem. Soc. Rev.*, 2016, **45**, 5589–5604.
10 G. Fichman and E. Gazit, *Acta Biomater.*, 2014, **10**, 1671–1682.
11 E. Mattia and S. Otto, *Nat. Nanotechnol.*, 2015, **10**, 111–119.
12 D. C. Sherrington and K. A. Taskinen, *Chem. Soc. Rev.*, 2001, **30**, 83–93.
13 Y. Shen, Y. Wang, I. W. Hamley, W. Qi, R. Su and Z. He, *Prog. Polym. Sci.*, 2021, **123**, 101469.
14 Y. Zheng, K. Mao, S. Chen and H. Zhu, *Front. Bioeng. Biotechnol.*, 2021, **9**, 703004.
15 V. Apostolopoulos, J. Bojarska, T.-T. Chai, S. Elnagdy, K. Kaczmarek, J. Matsoukas, R. New, K. Parang, O. P. Lopez, H. Parhiz, C. O. Perera, M. Pickholz, M. Remko, M. Saviano, M. Skwarczynski, Y. Tang, W. M. Wolf, T. Yoshiya, J. Zabrocki, P. Zielenkiewicz, M. AlKhazindar, V. Barriga, K. Kelaidonis, E. M. Sarasia and I. Toth, *Molecules*, 2021, **26**, 430.
16 R. Perlikowska, *Peptides*, 2021, **140**, 170528.
17 L. Schnaider, L. Shimonov, T. Kreiser, D. Zaguri, D. Bychenko, I. Brickner, S. Kolusheva, A. Lichtenstein, J. Kost and E. Gazit, *ACS Appl. Bio Mater.*, 2020, **3**, 8395–8401.
18 A. Arul, S. Sivagnanam, A. Dey, O. Mukherjee, S. Ghosh and P. Das, *RSC Adv.*, 2020, **10**, 13420–13429.
19 B. Gilboa, C. Lafargue, A. Handelman, L. J. W. Shimon, G. Rosenman, J. Zyss and T. Ellenbogen, *Adv. Sci.*, 2017, **4**, 1700052.
20 B. Xue, M. Qin, T. Wang, J. Wu, D. Luo, Q. Jiang, Y. Li, Y. Cao and W. Wang, *Adv. Funct. Mater.*, 2016, **26**, 9053–9062.
21 Y. Shen, Y. Wang, I. W. Hamley, W. Qi, R. Su and Z. He, *Prog. Polym. Sci.*, 2021, **123**, 101469.
22 U. J. Meierhenrich, *Eur. Rev.*, 2013, **21**, 190–199.
23 V. S. Lamzin, Z. Dauter and K. S. Wilson, *Curr. Opin. Struct. Biol.*, 1995, **5**, 830–836.
24 H. G. Brittain, *J. Pharm. Biomed. Anal.*, 1998, **17**, 933–940.
25 A. Gogoi, S. Konwer and G.-Y. Zhuo, *Front. Chem.*, 2020, **8**, 611833.
26 D. Kondepudi, in *Chiral Analysis*, ed. P. L. Polavarapu, Elsevier, 2nd edn, 2018, pp. 3–28.
27 P. L. Polavarapu, *Tetrahedron: Asymmetry*, 1997, **8**, 3397–3401.
28 P. L. Polavarapu, *Molecules*, 2016, **21**, 1056.
29 L. A. Nafie, *Vibrational Optical Activity: Principles and Applications*, Wiley, 2011.
30 K. Ng, T. J. Edkins and D. R. Bobbitt, *Chirality*, 1999, **11**, 187–194.
31 C. Meinert, J. H. Bredehöft, J.-J. Filippi, Y. Baraud, L. Nahon, F. Wien, N. C. Jones, S. V. Hoffmann and U. J. Meierhenrich, *Angew. Chem., Int. Ed.*, 2012, **51**, 4484–4487.
32 P. J. Stephens, F. J. Devlin and J.-J. Pan, *Chirality*, 2008, **20**, 643–663.
33 H. Yamagishi, H. Sato and I. Kawamura, *Chirality*, 2021, **33**, 652–659.
34 D. Kurouski, *Anal. Chim. Acta*, 2017, **990**, 54–66.
35 J. M. Bijvoet, A. F. Peerdeman and A. J. van Bommel, *Nature*, 1951, **168**, 271–272.
36 A. L. Thompson and D. J. Watkin, *Tetrahedron: Asymmetry*, 2009, **20**, 712–717.
37 H. D. Flack, *Chimia*, 2014, **68**, 26.
38 H. D. Flack and G. Bernardinelli, *Chirality*, 2008, **20**, 681–690.
39 S. Parsons, *Tetrahedron: Asymmetry*, 2017, **28**, 1304–1313.
40 *Determination of Absolute and Relative Configuration: 4.2. Determination of Absolute and Relative Configuration by X-ray and Neutron Diffraction Methods*, Thieme Verlag, 4th edn, 1995.
41 H. D. Flack, *Acta Crystallogr., Sect. A:Found. Crystallogr.*, 1983, **39**, 876–881.
42 J. R. Deschamps, *Life Sci.*, 2010, **86**, 585–589.
43 V. Kumar Vashistha, *Asian J. Org. Chem.*, 2022, **11**, e202200544.
44 C. Aroulanda and P. Lesot, *Chirality*, 2022, **34**, 182–244.
45 D. Parker, *Chem. Rev.*, 1991, **91**, 1441–1457.
46 T. J. Wenzel, *Differentiation of Chiral Compounds Using NMR Spectroscopy*, John Wiley & Sons, Ltd, 2018, pp. i–xxi.
47 D. Leung, S. O. Kang and E. V. Anslyn, *Chem. Soc. Rev.*, 2011, **41**, 448–479.
48 M. P. Williamson and J. P. Waltho, *Chem. Soc. Rev.*, 1992, **21**, 227–236.
49 V. Kumar Vashistha, *Asian J. Org. Chem.*, 2022, **11**, e202200544.
50 P. L. Rinaldi, *Prog. Nucl. Magn. Reson. Spectrosc.*, 1982, **15**, 291–352.
51 T. J. Wenzel and C. D. Chisholm, *Chirality*, 2011, **23**, 190–214.
52 R. R. Groleau, M. E. Powell, C. D. Evans, P. S. Fordred, S. D. Bull and T. D. James, in *Comprehensive Chirality*, ed. J. Cossy, Academic Press, Oxford, 2nd edn, 2024, pp. 593–631.
53 J. M. Seco, E. Quiñoá and R. Riguera, *Chem. Rev.*, 2004, **104**, 17–118.
54 J. M. Seco, E. Quiñoá and R. Riguera, *Chem. Rev.*, 2012, **112**, 4603–4641.
55 F. Balzano, A. Iuliano, G. Uccello-Barretta and V. Zullo, *J. Org. Chem.*, 2022, **87**, 12698–12709.
56 W. H. Pirkle, D. L. Sikkenga and M. S. Pavlin, *J. Org. Chem.*, 1977, **42**, 384–387.
57 J. A. Dale, D. L. Dull and H. S. Mosher, *J. Org. Chem.*, 1969, **34**, 2543–2549.
58 J. M. Seco, E. Quiñoá and R. Riguera, *Tetrahedron: Asymmetry*, 2001, **12**, 2915–2925.
59 M. Malinowska, S. Jarzyński, A. Pieczonka, M. Rachwalski, S. Leśniak and A. Zawisza, *J. Org. Chem.*, 2020, **85**, 11794–11801.

60 J. Wen, L. Feng, H. Zhao, L. Zheng, P. Stavropoulos, L. Ai and J. Zhang, *J. Org. Chem.*, 2022, **87**, 7934–7944.
61 Z. Sun, Z. Chen, Y. Wang, X. Zhang, J. Xu, G. Bian and L. Song, *Org. Lett.*, 2020, **22**, 589–593.
62 J. Yang, B. Chatelet, V. Dufaud, D. Hérault, M. Jean, N. Vanthuyne, J.-C. Mulatier, D. Pitrat, L. Guy, J.-P. Dutasta and A. Martinez, *Org. Lett.*, 2020, **22**, 891–895.
63 S. Jang and H. Kim, *Asian J. Org. Chem.*, 2021, **10**, 886–890.
64 I. Louzao, J. M. Seco, E. Quiñoá and R. Riguera, *Chem. Commun.*, 2010, **46**, 7903–7905.
65 M. Pérez-Trujillo, E. Monteagudo and T. Parella, *Anal. Chem.*, 2013, **85**, 10887–10894.
66 D. Prasad, S. Mogurampelly and S. R. Chaudhari, *RSC Adv.*, 2020, **10**, 2303–2312.
67 M. Palomino-Schätzlein, A. Virgili, S. Gil and C. Jaime, *J. Org. Chem.*, 2006, **71**, 8114–8120.
68 M. S. Silva, *Molecules*, 2017, **22**, 247.
69 Y. Jia, L. Wen, W. Bao, Z. Xu, J. Wu and Y. Zhao, *Anal. Chem.*, 2023, **95**, 10362–10367.
70 H. Li, Z. Xu, S. Zhang, Y. Jia and Y. Zhao, *Anal. Chem.*, 2022, **94**, 2023–2031.
71 J. Liang, Z. Xu, J. Wu and Y. Zhao, *Anal. Chem.*, 2023, **95**, 7569–7574.
72 O. N. Gorunova, I. M. Novitskiy, Y. K. Grishin, I. P. Gloriozov, V. A. Roznyatovsky, V. N. Khrustalev, K. A. Kochetkov and V. V. Dunina, *Organometallics*, 2016, **35**, 75–90.
73 Y. Zhao and T. M. Swager, *J. Am. Chem. Soc.*, 2015, **137**, 3221–3224.
74 Z. Xu and Y. Zhao, *J. Fluorine Chem.*, 2023, **266**, 110089.
75 D.-Q. Han and Z.-P. Yao, *TrAC, Trends Anal. Chem.*, 2020, **123**, 115763.
76 P. Dwivedi, C. Wu, L. M. Matz, B. H. Clowers, W. F. Siems and H. H. Hill, *Anal. Chem.*, 2006, **78**, 8200–8206.
77 A. Mie, M. Jörntén-Karlsson, B.-O. Axelsson, A. Ray and C. T. Reimann, *Anal. Chem.*, 2007, **79**, 2850–2858.
78 V. Domalain, M. Hubert-Roux, V. Tognetti, L. Joubert, C. M. Lange, J. Rouden and C. Afonso, *Chem. Sci.*, 2014, **5**, 3234–3239.
79 R. Pérez-Míguez, B. Bruyneel, M. Castro-Puyana, M. L. Marina, G. W. Somsen and E. Domínguez-Vega, *Anal. Chem.*, 2019, **91**, 3277–3285.
80 J. M. Will, A. Behrens, M. Macke, C. D. Quarles and U. Karst, *Anal. Chem.*, 2021, **93**, 878–885.
81 P. Krüger and K.-M. Weitzel, *Angew. Chem., Int. Ed.*, 2021, **60**, 17861–17865.
82 S. O. Fakayode, A. A. Williams, M. A. Busch, K. W. Busch and I. M. Warner, *J. Fluoresc.*, 2006, **16**, 659–670.
83 O. Rusin, O. Alpturk, M. He, J. O. Escobedo, S. Jiang, F. Dawan, K. Lian, M. E. McCarroll, I. M. Warner and R. M. Strongin, *J. Fluoresc.*, 2004, **14**, 611–615.
84 O. Rusin, V. Král, J. O. Escobedo and R. M. Strongin, *Org. Lett.*, 2004, **6**, 1373–1376.
85 A. Belardini, E. Petronijevic, R. Ghahri, D. Rocco, F. Pandolfi, C. Sibilia and L. Mattiello, *Appl. Sci.*, 2021, **11**, 11375.
86 L. Pu, *Acc. Chem. Res.*, 2017, **50**, 1032–1040.
87 Y.-Y. Zhu, X.-D. Wu, S.-X. Gu and L. Pu, *J. Am. Chem. Soc.*, 2019, **141**, 175–181.
88 B. Valeur and M. N. Berberan-Santos, *Molecular Fluorescence: Principles and Applications*, John Wiley & Sons, Ltd, 2012.
89 D. Frackowiak, *J. Photochem. Photobiol., B*, 1988, **2**, 399.
90 I. P. Silvestri and P. J. J. Colbon, *ACS Med. Chem. Lett.*, 2021, **12**, 1220–1229.
91 G. L. Thejashree, E. Doris, E. Gravel and I. N. N. Namboothiri, *Eur. J. Org. Chem.*, 2022, e202201035.
92 M. Morvan and I. Mikšík, *Separations*, 2021, **8**, 112.
93 T. Miyamoto and H. Homma, *Biochim. Biophys. Acta, Proteins Proteomics*, 2018, **1866**, 775–782.
94 V. Kasicka, *Electrophoresis*, 2022, **43**, 82–108.
95 R. Dominguez, B. Serra, A. J. Reviejo and J. M. Pingarron, *Anal. Biochem.*, 2001, **298**, 275–282.
96 L. Zhang, G. Wang, C. Xiong, L. Zheng, J. He, Y. Ding, H. Lu, G. Zhang, K. Cho and L. Qiu, *Biosens. Bioelectron.*, 2018, **105**, 121–128.
97 Y. Zhou, B. Yu and K. Levon, *Chem. Mater.*, 2003, **15**, 2774–2779.
98 T. Polenova, R. Gupta and A. Goldbourt, *Anal. Chem.*, 2015, **87**, 5458–5469.
99 R. Tycko, *Annu. Rev. Phys. Chem.*, 2001, **52**, 575–606.
100 M. Bonaccorsi, T. Le Marchand and G. Pintacuda, *Curr. Opin. Struct. Biol.*, 2021, **70**, 34–43.
101 P. J. Chu, M. J. Potrzebowski, A. I. Scott and Y. Gao, *J. Am. Chem. Soc.*, 1990, **112**, 881–883.
102 M. M. Słabicki, M. J. Potrzebowski, G. Bujacz, S. Olejniczak and J. Olczak, *J. Phys. Chem. B*, 2004, **108**, 4535–4545.
103 B. Reif, S. E. Ashbrook, L. Emsley and M. Hong, *Nat. Rev. Methods Primers*, 2021, **1**, 1–23.
104 M. Deschamps, in *Annual Reports on NMR Spectroscopy*, ed. G. A. Webb, Academic Press, 2014, vol. 81, pp. 109–144.
105 Y. Nishiyama, G. Hou, V. Agarwal, Y. Su and A. Ramamoorthy, *Chem. Rev.*, 2023, **123**, 918–988.
106 M. K. Dudek, S. Kaźmierski and M. J. Potrzebowski, in *Annual Reports on NMR Spectroscopy*, ed. G. A. Webb, Academic Press, 2021, vol. 103, pp. 97–189.
107 E. O. Stejskal, J. Schaefer and J. S. Waugh, *J. Magn. Reson.*, 1977, **28**, 105–112.
108 H. Farooq, D. Courtier-Murias, R. Soong, W. Bermel, W. M. Kingery and A. J. Simpson, *Curr. Org. Chem.*, 2013, **17**, 3013–3031.
109 N. Sengupta, H. Maekawa, W. Zhuang, C. Toniolo, S. Mukamel, D. J. Tobias and N.-H. Ge, *J. Phys. Chem. B*, 2009, **113**, 12037–12049.
110 V. Cervetto, P. Hamm and J. Helbing, *J. Phys. Chem. B*, 2008, **112**, 8398–8405.
111 H. Kong, X. Sun, L. Yang, X. Liu, H. Yang and R.-H. Jin, *Anal. Chem.*, 2020, **92**, 14292–14296.
112 V. Parchaňský, J. Kapitán and P. Bouř, *RSC Adv.*, 2014, **4**, 57125–57136.
113 V. Parchaňský, J. Kapitán, J. Kaminský, J. Šebestík and P. Bouř, *J. Phys. Chem. Lett.*, 2013, **4**, 2763–2768.

114 G. H. Beaven and E. R. Holiday, in *Advances in Protein Chemistry*, ed. M. L. Anson, K. Bailey and J. T. Edsall, Academic Press, 1952, vol. 7, pp. 319–386.
115 L. Yang, F. Luo and W. Wei, *Anal. Methods*, 2021, **13**, 1905–1910.
116 L. Huang, X. Zhang, C. Xu, J. Wang, A. Zhang, Y. Liu and H. Zhu, *Adv. Opt. Mater.*, 2025, 2500053.
117 K. Makabe, D. McElheny, V. Tereshko, A. Hilyard, G. Gawlak, S. Yan, A. Koide and S. Koide, *Proc. Natl. Acad. Sci. U. S. A.*, 2006, **103**, 17753–17758.
118 I. Bak-Sypien, T. Pawlak, P. Paluch, A. Wroblewska, R. Dolot, A. Pawlowicz, M. Szczesio, E. Wielgus, S. Kaźmierski, M. Górecki, R. Pawlowska, A. Chworos and M. J. Potrzebowski, *Sci. Rep.*, 2024, **14**, 12825.
119 I. W. Hamley and V. Castelletto, *Adv. Colloid Interface Sci.*, 2023, **318**, 102959.
120 T. Narayanan, A. Rüter and U. Olsson, *Front. Bioeng. Biotechnol.*, 2021, **9**, 654339.
121 T. Gulik-Krzywicki, C. Fouquey and J. Lehn, *Proc. Natl. Acad. Sci. U. S. A.*, 1993, **90**, 163–167.
122 F. Schulz, I. Lokteva, W. J. Parak and F. Lehmkühler, *Part. Part. Syst. Charact.*, 2021, **38**, 2100087.
123 R. Kubota, W. Tanaka and I. Hamachi, *Chem. Rev.*, 2021, **121**, 14281–14347.
124 J. W. Smith and Q. Chen, *J. Mater. Chem. B*, 2020, **8**, 8490–8506.
125 K. M. Yip, N. Fischer, E. Paknia, A. Chari and H. Stark, *Nature*, 2020, **587**, 157–161.
126 T. Nakane, A. Kotecha, A. Sente, G. McMullan, S. Masiulis, P. M. G. E. Brown, I. T. Grigoras, L. Malinauskaite, T. Malinauskas, J. Miehling, T. Uchański, L. Yu, D. Karia, E. V. Pechnikova, E. de Jong, J. Keizer, M. Bischoff, J. McCormack, P. Tiemeijer, S. W. Hardwick, D. Y. Chirgadze, G. Murshudov, A. R. Aricescu and S. H. W. Scheres, *Nature*, 2020, **587**, 152–156.
127 J. Harapin, M. Eibauer and O. Medalia, *Structure*, 2013, **21**, 1522–1530.
128 K. C. Bustillo, S. E. Zeltmann, M. Chen, J. Donohue, J. Ciston, C. Ophus and A. M. Minor, *Acc. Chem. Res.*, 2021, **54**, 2543–2551.
129 K. Bian, C. Gerber, A. J. Heinrich, D. J. Müller, S. Scheuring and Y. Jiang, *Nat. Rev. Methods Primers*, 2021, **1**, 1–29.
130 P. K. Hansma, V. B. Elings, O. Marti and C. E. Bracker, *Science*, 1988, **242**, 209–216.
131 K. Skorupska, D. J. Smith, D. S. A. Campbell, H. Jungblut and J. J. L. Hans, *ECS Trans.*, 2007, **2**, 63.
132 L.-P. Xu, Y. Liu and X. Zhang, *Nanoscale*, 2011, **3**, 4901–4915.
133 B. Hou, T. Zhang, H. Yang, X. Han, L. Liu, L. Li, C. Grazioli, X. Wu, N. Jiang and Y. Wang, *Interdiscip. Mater.*, 2023, **2**, 511–528.
134 J. A. A. W. Elemans, I. D. Cat, H. Xu and S. D. Feyter, *Chem. Soc. Rev.*, 2009, **38**, 722–736.
135 M. Mura, F. Silly, G. A. D. Briggs, M. R. Castell and L. N. Kantorovich, *J. Phys. Chem. C*, 2009, **113**, 21840–21848.
136 T. Kudernac, S. Lei, J. A. A. W. Elemans and S. D. Feyter, *Chem. Soc. Rev.*, 2009, **38**, 402–421.
137 A. Rodríguez-Galván and F. F. Contreras-Torres, *Nanomaterials*, 2022, **12**, 3013.
138 M. Nasrollahzadeh, M. Atarod, M. Sajjadi, S. M. Sajadi and Z. Issaabadi, in *Interface Science and Technology*, ed. M. Nasrollahzadeh, S. M. Sajadi, M. Sajjadi, Z. Issaabadi and M. Atarod, Elsevier, 2019, vol. 28, pp. 199–322.
139 S. Maity, J. Ottelé, G. M. Santiago, P. W. J. M. Frederix, P. Kroon, O. Markovitch, M. C. A. Stuart, S. J. Marrink, S. Otto and W. H. Roos, *J. Am. Chem. Soc.*, 2020, **142**, 13709–13717.
140 M. Manrho, S. R. Krishnaswamy, B. Kriete, I. Patmanidis, A. H. de Vries, S. J. Marrink, T. L. C. Jansen, J. Knoester and M. S. Pshenichnikov, *J. Am. Chem. Soc.*, 2023, **145**, 22494–22503.
141 V. G. Gisbert, S. Benaglia, M. R. Uhlig, R. Proksch and R. Garcia, *ACS Nano*, 2021, **15**, 1850–1857.
142 C.-C. Hsu, J. Xu, B. Brinkhof, H. Wang, Z. Cui, W. E. Huang and H. Ye, *Proc. Natl. Acad. Sci. U. S. A.*, 2020, **117**, 18412–18423.
143 F. Palombo, F. Tamagnini, J. C. G. Jeynes, S. Mattana, I. Swift, J. Nallala, J. Hancock, J. T. Brown, A. D. Randall and N. Stone, *Analyst*, 2018, **143**, 850–857.
144 P. W. J. M. Frederix, R. V. Ulijn, N. T. Hunt and T. Tuttle, *J. Phys. Chem. Lett.*, 2011, **2**, 2380–2384.
145 P. W. J. M. Frederix, G. G. Scott, Y. M. Abul-Haija, D. Kalafatovic, C. G. Pappas, N. Javid, N. T. Hunt, R. V. Ulijn and T. Tuttle, *Nat. Chem.*, 2015, **7**, 30–37.
146 S. J. Marrink, H. J. Risselada, S. Yefimov, D. P. Tieleman and A. H. de Vries, *J. Phys. Chem. B*, 2007, **111**, 7812–7824.
147 L. Monticelli, S. K. Kandasamy, X. Periole, R. G. Larson, D. P. Tieleman and S.-J. Marrink, *J. Chem. Theory Comput.*, 2008, **4**, 819–834.
148 P. Hosseinzadeh, G. Bhardwaj, V. K. Mulligan, M. D. Shortridge, T. W. Craven, F. Pardo-Avila, S. A. Rettie, D. E. Kim, D.-A. Silva, Y. M. Ibrahim, I. K. Webb, J. R. Cort, J. N. Adkins, G. Varani and D. Baker, *Science*, 2017, **358**, 1461–1466.
149 V. K. Mulligan, C. S. Kang, M. R. Sawaya, S. Rettie, X. Li, I. Antselovich, T. W. Craven, A. M. Watkins, J. W. Labonte, F. DiMaio, T. O. Yeates and D. Baker, *Protein Sci.*, 2020, **29**, 2433–2445.
150 I. V. Likhachev and V. S. Bystrov, *Math. Biol. Bioinf.*, 2021, **16**, 244–255.
151 V. Bystrov, I. Likhachev, A. Sidorova, S. Filippov, A. Lutsenko, D. Shpigun and E. Belova, *Nanomaterials*, 2022, **12**, 861.
152 P. Zhou, L. Deng, Y. Wang, J. R. Lu and H. Xu, *Langmuir*, 2016, **32**, 4662–4672.
153 P. Zhou, X. Hu, J. Li, Y. Wang, H. Yu, Z. Chen, D. Wang, Y. Zhao, S. M. King, S. E. Rogers, J. Wang, J. R. Lu and H. Xu, *J. Am. Chem. Soc.*, 2022, **144**, 21544–21554.
154 Z. Liu, J. Wang, Y. Luo, S. Zhao, W. Li and S. Z. Li, *Briefings Bioinf.*, 2023, **24**, bbad409.
155 Z. Yang, S. K. Yorke, T. P. J. Knowles and M. J. Buehler, *Sci. Adv.*, 2025, **11**, eadv1971.
156 E. Dražić, D. Jelušić, P. Janković Bevandić, G. Mauša and D. Kalafatovic, *ACS Nano*, 2025, **19**, 20295–20320.

157 C. Yan, A. Altunbas, T. Yucel, R. P. Nagarkar, J. P. Schneider and D. J. Pochan, *Soft Matter*, 2010, **6**, 5143–5156.
158 J. K. Wychowaniec, A. M. Smith, C. Ligorio, O. O. Mykhaylyk, A. F. Miller and A. Saiani, *Biomacromolecules*, 2020, **21**, 2285–2297.
159 K.-H. Ernst, *Chimia*, 2018, **72**, 399.
160 C. P. Brock, W. B. Schweizer and J. D. Dunitz, *J. Am. Chem. Soc.*, 1991, **113**, 9811–9820.
161 J. D. Dunitz and A. Gavezzotti, *J. Phys. Chem. B*, 2012, **116**, 6740–6750.
162 C. Yuan, W. Ji, R. Xing, J. Li, E. Gazit and X. Yan, *Nat. Rev. Chem.*, 2019, **3**, 567–588.
163 C. H. Görbitz, *Chem. - Eur. J.*, 2001, **7**, 5153–5159.
164 M. Reches and E. Gazit, *Science*, 2003, **300**, 625–627.
165 M. Reches and E. Gazit, *Nano Lett.*, 2004, **4**, 581–585.
166 N. Kol, L. Adler-Abramovich, D. Barlam, R. Z. Shneck, E. Gazit and I. Rousso, *Nano Lett.*, 2005, **5**, 1343–1346.
167 S. Marchesan, A. V. Vargiu and K. E. Styan, *Molecules*, 2015, **20**, 19775–19788.
168 J.-H. Lee, K. Heo, K. Schulz-Schönhagen, J. H. Lee, M. S. Desai, H.-E. Jin and S.-W. Lee, *ACS Nano*, 2018, **12**, 8138–8144.
169 E. Mayans and C. Alemán, *Molecules*, 2020, **25**, 6037.
170 H. Erdoğan, *Soft Matter*, 2021, **17**, 5221–5230.
171 P. M. Rodger, C. Montgomery, G. Costantini and A. Rodger, *Phys. Chem. Chem. Phys.*, 2021, **23**, 4597–4604.
172 P. S. Zelenovskiy, A. S. Nuraeva, S. Kopyl, S. G. Arkhipov, S. G. Vasilev, V. S. Bystrov, D. A. Gruzdev, M. Waliczek, V. Svitlyk, V. Ya. Shur, L. Mafra and A. L. Kholkin, *Cryst. Growth Des.*, 2019, **19**, 6414–6421.
173 V. S. Bystrov, P. S. Zelenovskiy, A. S. Nuraeva, S. Kopyl, O. A. Zhulyabina and V. A. Tverdislov, *J. Mol. Model.*, 2019, **25**, 199.
174 Advancing Structural Science | CCDC, **https://www.ccdc.cam.ac.uk/**, (accessed 21 March 2025).
175 T. O. Mason, D. Y. Chirgadze, A. Levin, L. Adler-Abramovich, E. Gazit, T. P. J. Knowles and A. K. Buell, *ACS Nano*, 2014, **8**, 1243–1253.
176 P. S. Zelenovskii, K. Romanyuk, M. S. Liberato, P. Brandão, F. F. Ferreira, S. Kopyl, L. M. Mafra, W. A. Alves and A. L. Kholkin, *Adv. Funct. Mater.*, 2021, **31**, 2102524.
177 E. Scarel, M. De Corti, M. Polentarutti, G. Pierri, C. Tedesco and S. Marchesan, *J. Pept. Sci.*, 2024, **30**, e3559.
178 C. H. Görbitz, *Acta Crystallogr., Sect. C:Cryst. Struct. Commun.*, 1997, **53**, 736–739.
179 C. H. Görbitz, E. Gundersen, F. Teixidor, C. Viñas, M. M. Abad, R. I. Nielsen, C. E. Olsen, C. N. Rosendahl, M. Haugg, N. Trabesinger-Rüf and E. G. Weinhold, *Acta Chem. Scand.*, 1996, **50**, 537–543.
180 S. N. Mitra and E. Subramanian, *Biopolymers*, 1994, **34**, 1139–1143.
181 G. Dolai, R. S. Giri, S. Roy and B. Mandal, *Pept. Sci.*, 2021, **113**, e24229.
182 S. Roy, R. S. Giri, G. Dolai and B. Mandal, *J. Mol. Struct.*, 2020, **1221**, 128877.
183 R. S. Giri, S. Pal, S. Roy, G. Dolai, S. R. Manne, S. Paul and B. Mandal, *Pept. Sci.*, 2021, **113**, e24176.
184 A. Jeziorna, K. Stopczyk, E. Skorupska, K. Luberda-Durnas, M. Oszajca, W. Lasocha, M. Górecki, J. Frelek and M. J. Potrzebowski, *Cryst. Growth Des.*, 2015, **15**, 5138–5148.
185 A. Chotera-Ouda, A. Jeziorna, S. Kaźmierski, R. Dolot, M. K. Dudek and M. J. Potrzebowski, *Chem. – Eur. J.*, 2022, **28**, e202202005.
186 M. Jaworska, A. Jeziorna, E. Drabik and M. J. Potrzebowski, *J. Phys. Chem. C*, 2012, **116**, 12330–12338.
187 A. N. Rissanou, E. Georgilis, E. Kasotakis, A. Mitraki and V. Harmandaris, *J. Phys. Chem. B*, 2013, **117**, 3962–3975.
188 P. Makam and E. Gazit, *Chem. Soc. Rev.*, 2018, **47**, 3406–3420.
189 S. Kralj, O. Bellotto, E. Parisi, A. M. Garcia, D. Iglesias, S. Semeraro, C. Deganutti, P. D'Andrea, A. V. Vargiu, S. Geremia, R. De Zorzi and S. Marchesan, *ACS Nano*, 2020, **14**, 16951–16961.
190 A. M. Garcia, M. Melchionna, O. Bellotto, S. Kralj, S. Semeraro, E. Parisi, D. Iglesias, P. D'Andrea, R. De Zorzi, A. V. Vargiu and S. Marchesan, *ACS Nano*, 2021, **15**, 3015–3025.
191 B. Chatterjee, I. Saha, S. Raghothama, S. Aravinda, R. Rai, N. Shamala and P. Balaram, *Chem. - Eur. J.*, 2008, **14**, 6192–6204.
192 I. Saha and N. Shamala, *Biopolymers*, 2012, **97**, 54–64.
193 R. Rai, S. Aravinda, K. Kanagarajadurai, S. Raghothama, N. Shamala and P. Balaram, *J. Am. Chem. Soc.*, 2006, **128**, 7916–7928.
194 S. Shaham-Niv, L. Adler-Abramovich, L. Schnaider and E. Gazit, *Sci. Adv.*, 2015, **1**, e1500137.
195 P. Singh, S. K. Brar, M. Bajaj, N. Narang, V. S. Mithu, O. P. Katare, N. Wangoo and R. K. Sharma, *Mater. Sci. Eng., C*, 2017, **72**, 590–600.
196 S. Shaham-Niv, P. Rehak, L. Vuković, L. Adler-Abramovich, P. Král and E. Gazit, *Isr. J. Chem.*, 2017, **57**, 729–737.
197 D. Banik, S. Kundu, P. Banerjee, R. Dutta and N. Sarkar, *J. Phys. Chem. B*, 2017, **121**, 1533–1543.
198 S. Bera, B. Xue, P. Rehak, G. Jacoby, W. Ji, L. J. W. Shimon, R. Beck, P. Král, Y. Cao and E. Gazit, *ACS Nano*, 2020, **14**, 1694–1706.
199 A. K. Mondal, N. Brown, S. Mishra, P. Makam, D. Wing, S. Gilead, Y. Wiesenfeld, G. Leitus, L. J. W. Shimon, R. Carmieli, D. Ehre, G. Kamieniarz, J. Fransson, O. Hod, L. Kronik, E. Gazit and R. Naaman, *ACS Nano*, 2020, **14**, 16624–16633.
200 B. P. Bloom, Y. Paltiel, R. Naaman and D. H. Waldeck, *Chem. Rev.*, 2024, **124**, 1950–1991.
201 S. Lin, Q. Tong, P. Jiang, B. Li, Y. Li and Y. Yang, *New J. Chem.*, 2021, **45**, 12585–12592.
202 O. Bellotto, G. Pierri, P. Rozhin, M. Polentarutti, S. Kralj, P. D'Andrea, C. Tedesco and S. Marchesan, *Org. Biomol. Chem.*, 2022, **20**, 6211–6218.
203 O. Bellotto, S. Kralj, R. D. Zorzi, S. Geremia and S. Marchesan, *Soft Matter*, 2020, **16**, 10151–10157.
204 S. Marchesan, C. D. Easton, K. E. Styan, L. J. Waddington, F. Kushkaki, L. Goodall, K. M. McLean, J. S. Forsythe and P. G. Hartley, *Nanoscale*, 2014, **6**, 5172–5180.

205 S. Marchesan, L. Waddington, C. D. Easton, D. A. Winkler, L. Goodall, J. Forsythe and P. G. Hartley, *Nanoscale*, 2012, **4**, 6752–6760.
206 A. M. Garcia, D. Iglesias, E. Parisi, K. E. Styan, L. J. Waddington, C. Deganutti, R. De Zorzi, M. Grassi, M. Melchionna, A. V. Vargiu and S. Marchesan, *Chem*, 2018, **4**, 1862–1876.
207 S. Marchesan, K. E. Styan, C. D. Easton, L. Waddington and A. V. Vargiu, *J. Mater. Chem. B*, 2015, **3**, 8123–8132.
208 M. C. Mañas-Torres, P. Alletto, S. Adorinni, A. V. Vargiu, L. Á. de Cienfuegos and S. Marchesan, *Org. Biomol. Chem.*, 2025, **23**, 2797–2801.
209 C. G. Pappas, P. W. J. M. Frederix, T. Mutasa, S. Fleming, Y. M. Abul-Haija, S. M. Kelly, A. Gachagan, D. Kalafatovic, J. Trevino, R. V. Ulijn and S. Bai, *Chem. Commun.*, 2015, **51**, 8465–8468.
210 B. Rosetti, E. Scarel, L. Colomina-Alfaro, S. Adorinni, G. Pierri, O. Bellotto, K. Mamprin, M. Polentarutti, A. Bandiera, C. Tedesco and S. Marchesan, *Polymers*, 2022, **14**, 4554.
211 T. G. Meikle, C. E. Conn, F. Separovic and C. J. Drummond, *RSC Adv.*, 2016, **6**, 68685–68694.
212 K. Tatsuta, *J. Antibiot.*, 2013, **66**, 107–129.
213 K. Hamamoto, Y. Kida, Y. Zhang, T. Shimizu and K. Kuwano, *Microbiol. Immunol.*, 2002, **46**, 741–749.
214 C. Zhong, S. Gou, T. Liu, Y. Zhu, N. Zhu, H. Liu, Y. Zhang, J. Xie, X. Guo and J. Ni, *Microb. Pathog.*, 2020, **139**, 103871.
215 H. Wang, Z. Feng and B. Xu, *Adv. Drug Delivery Rev.*, 2017, **110–111**, 102–111.
216 Y. Zhou, Y. Zou, M. Yang, S. Mei, X. Liu, H. Han, C.-D. Zhang and M.-M. Niu, *J. Am. Chem. Soc.*, 2022, **144**, 7117–7128.
217 S. Muller Benkirane, N. Guichard, G. Regenmortel, M. H. V. Van and F. Brown, *Expert Opin. Invest. Drugs*, 1998, **7**, 1429–1438.
218 Z. Feng and B. Xu, *Biomol. Concepts*, 2016, **7**, 179–187.
219 L. Zhao and W. Lu, *Curr. Opin. Chem. Biol.*, 2014, **22**, 56–61.
220 S. Kapil and V. Sharma, *Can. J. Microbiol.*, 2021, **67**, 119–137.
221 O. Bellotto, S. Semeraro, A. Bandiera, F. Tramer, N. Pavan and S. Marchesan, *Pharmaceutics*, 2022, **14**, 446.
222 M. Seia and E. Zisman, *FASEB J.*, 1997, **11**, 449–456.
223 S. A. Fuchs, R. Berger, L. W. J. Klomp and T. J. de Koning, *Mol. Genet. Metab.*, 2005, **85**, 168–180.
224 J. J. A. J. Bastings, H. M. van Eijk, S. W. Olde Damink and S. S. Rensen, *Nutrients*, 2019, **11**, 2205.
225 W. K. Restu, Y. Nishida, S. Yamamoto, J. Ishii and T. Maruyama, *Langmuir*, 2018, **34**, 8065–8074.
226 W. K. Restu, S. Yamamoto, Y. Nishida, H. Ienaga, T. Aoi and T. Maruyama, *Mater. Sci. Eng., C*, 2020, **111**, 110746.
227 A. Agrawal, E. M. Euliano, B. H. Pogostin, M. H. Yu, J. W. R. Swain, J. D. Hartgerink and K. J. McHugh, *Cel. Mol. Bioeng.*, 2024, **17**, 441–451.
228 Z. Luo, Q. Wu, C. Yang, H. Wang, T. He, Y. Wang, Z. Wang, H. Chen, X. Li, C. Gong and Z. Yang, *Adv. Mater.*, 2017, **29**, 1601776.
229 J. Ding, T. Wang, Z. Lin, Z. Li, J. Yang, F. Li, Y. Rong, X. Chen and C. He, *Nat. Commun.*, 2025, **16**, 1222.
230 K. J. Nagy, M. C. Giano, A. Jin, D. J. Pochan and J. P. Schneider, *J. Am. Chem. Soc.*, 2011, **133**, 14975–14977.
231 T. Tan, Y. Hou, J. Shi, B. Wang and Y. Zhang, *Mater. Today Bio*, 2024, **25**, 100961.
232 I. J. Duti, J. R. Florian, A. R. Kittel, C. D. Amelung, V. P. Gray, K. J. Lampe and R. A. Letteri, *J. Am. Chem. Soc.*, 2023, **145**, 18468–18476.
233 D. Florio, C. Di Natale, P. L. Scognamiglio, M. Leone, S. La Manna, S. Di Somma, P. A. Netti, A. M. Malfitano and D. Marasco, *Bioorg. Chem.*, 2021, **114**, 105047.
234 S. Kuila, A. K. Singh, A. Shrivastava, S. Dey, T. Singha, L. Roy, B. Satpati and J. Nanda, *J. Phys. Chem. B*, 2023, **127**, 4808–4819.
235 K. McAulay, B. Dietrich, H. Su, M. T. Scott, S. Rogers, Y. K. Al-Hilaly, H. Cui, L. C. Serpell, A. M. Seddon, E. R. Draper and D. J. Adams, *Chem. Sci.*, 2019, **10**, 7801–7806.
236 R. R. Sonani, S. Bianco, B. Dietrich, J. Doutch, E. R. Draper, D. J. Adams and E. H. Egelman, *Cell Rep. Phys. Sci.*, 2024, **5**, 101812.
237 L. Wang, X. Jin, L. Ye, A. Zhang, D. Bezuidenhout and Z. Feng, *Langmuir*, 2017, **33**, 13821–13827.
238 M. Li, M. Liu, Y. Shang, C. Ren, J. Liu, H. Jin and Z. Wang, *RSC Adv.*, 2020, **10**, 13900–13906.
239 B. Adhikari, C. Singh, A. Shah, A. J. Lough and H.-B. Kraatz, *Chem. - Eur. J.*, 2015, **21**, 11560–11572.
240 G. Zhang, L. Zhang, H. Rao, Y. Wang, Q. Li, W. Qi, X. Yang, R. Su and Z. He, *J. Colloid Interface Sci.*, 2020, **577**, 388–396.
241 Z. Chen, Z. Lv, G. Qing and T. Sun, *J. Mater. Chem. B*, 2017, **5**, 3163–3171.
242 K. Shao, Z. Lv, Y. Xiong, G. Li, D. Wang, H. Zhang and G. Qing, *RSC Adv.*, 2019, **9**, 10360–10363.
243 X. Wang, C. Wei, J.-H. Su, B. He, G.-B. Wen, Y.-W. Lin and Y. Zhang, *Angew. Chem., Int. Ed.*, 2018, **57**, 3504–3508.
244 L. Ruckthong, A. F. A. Peacock, C. E. Pascoe, L. Hemmingsen, J. A. Stuckey and V. L. Pecoraro, *Chem. - Eur. J.*, 2017, **23**, 8232–8243.
245 G. Zhang, Y. Liang, Y. Wang, Q. Li, W. Qi, W. Zhang, R. Su and Z. He, *ACS Nano*, 2022, **16**, 6866–6877.
246 M. Conejero-Muriel, J. A. Gavira, E. Pineda-Molina, A. Belsom, M. Bradley, M. Moral, J. de, D. G.-L. Durán, A. L. González, J. J. Díaz-Mochón, R. Contreras-Montoya, Á. Martínez-Peragón, J. M. Cuerva and L. Á. de Cienfuegos, *Chem. Commun.*, 2015, **51**, 3862–3865.
247 M. Conejero-Muriel, R. Contreras-Montoya, J. J. Díaz-Mochón, L. Á. de Cienfuegos and J. A. Gavira, *CrystEngComm*, 2015, **17**, 8072–8078.
248 D. Gambhir, S. Kumar and R. R. Koner, *Soft Matter*, 2022, **18**, 3624–3637.
249 D. Yang, X. Li, Y.-F. Fan and D.-W. Zhang, *J. Am. Chem. Soc.*, 2005, **127**, 7996–7997.
250 A. Tripathi, A. Kumar and P. S. Pandey, *Tetrahedron Lett.*, 2012, **53**, 5745–5748.

251 F. Zhang, Z. Xu, S. Dong, L. Feng, A. Song, C.-H. Tung and J. Hao, *Soft Matter*, 2014, **10**, 4855–4862.
252 M. C. Mañas-Torres, C. Gila-Vilchez, J. A. González-Vera, F. Conejero-Lara, V. Blanco, J. Manuel Cuerva, M. T. Lopez-Lopez, A. Orte and L. Á. de Cienfuegos, *Mater. Chem. Front.*, 2021, **5**, 5452–5462.
253 X. Zhang, Z. Yang, J. Lin, W. Zhou, N. Sun and Y. Jia, *Int. J. Mol. Sci.*, 2025, **26**, 3998.
254 F. Auvray, D. Dennetiere, A. Giuliani, F. Jamme, F. Wien, B. Nay, S. Zirah, F. Polack, C. Menneglier, B. Lagarde, J. D. Hirst and M. Réfrégiers, *Struct. Dynam.*, 2019, **6**, 054307.
255 Z. Zhang, K. Chen, K. Tang, K. Chen, R. Li, X. Sun, Y. Hu, Q. Liu, M. Chen, H. Yang and X. Chen, *Anal. Chem.*, 2023, **95**, 4923–4931.
256 S. Wadhwa, D. Buyens and J. G. Korvink, *Adv. Mater.*, 2024, **36**, 2408547.